Amplification of *CRKL* Induces Transformation and Epidermal Growth Factor Receptor Inhibitor Resistance in Human Non–Small Cell Lung Cancers

Hiu Wing Cheung[1,6,9], Jinyan Du[2,9], Jesse S. Boehm[9], Frank He[2,9], Barbara A. Weir[1,9], Xiaoxing Wang[1,6,9], Mohit Butaney[1,3], Lecia V. Sequist[5,6], Biao Luo[9], Jeffrey A. Engelman[5,6], David E. Root[9], Matthew Meyerson[1,4,6,7,9], Todd R. Golub[2,4,6,9], Pasi A. Jänne[1,3,6], and William C. Hahn[1,4,6,8,9]

ABSTRACT

We previously identified a region of recurrent amplification on chromosome 22q11.21 in a subset of primary lung adenocarcinomas. Here we show that *CRKL*, encoding for an adaptor protein, is amplified and overexpressed in non–small cell lung cancer (NSCLC) cells that harbor 22q11.21 amplifications. Overexpression of CRKL in immortalized human airway epithelial cells promoted anchorage-independent growth and tumorigenicity. Oncogenic CRKL activates the SOS1-RAS-RAF-ERK and SRC-C3G-RAP1 pathways. Suppression of CRKL in NSCLC cells that harbor *CRKL* amplifications induced cell death. Overexpression of CRKL in epidermal growth factor receptor (*EGFR*)-mutant cells induces resistance to gefitinib by activating extracellular signal–regulated kinase and AKT signaling. We identified *CRKL* amplification in an EGFR inhibitor–treated lung adenocarcinoma that was not present before treatment. These observations demonstrate that CRKL overexpression induces cell transformation, credential CRKL as a therapeutic target for a subset of NSCLC that harbor *CRKL* amplifications, and implicate CRKL as an additional mechanism of resistance to EGFR-directed therapy.

SIGNIFICANCE: These studies credential *CRKL* as an oncogene in a subset of NSCLC. Overexpression of CRKL induces cell transformation and resistance to epidermal growth factor receptor inhibitor treatment and suggest that therapeutic interventions targeting CRKL may confer a clinical benefit in a defined subset of NSCLCs. *Cancer Discovery; 1(7);* 608–25. *©2011 AACR.*

INTRODUCTION

Although the prognosis for patients with non–small cell lung cancer (NSCLC) who present with late-stage disease remains poor, somatic mutations of the epidermal growth factor receptor (*EGFR*) serve as predictive biomarkers for both clinical response and survival in patients who receive EGFR inhibitors (1–7). Moreover, recent work indicates that mutations or translocations of the *ALK* tyrosine kinase also occur in a subset of NSCLC (8, 9) and that tumors that harbor such mutations are sensitive to ALK inhibitors (10, 11). Collectively, these studies suggest that identifying and characterizing genetic alterations in NSCLC will provide new targets for therapeutic strategies.

In previous work, researchers have identified 57 recurrent events of genomic gain or loss in primary NSCLC (12, 13). A small number of these recurrent genomic events has been found to harbor known and novel oncogenes and tumor suppressor genes, including amplification or mutation in *EGFR*, *KRAS*, *MYC*, *MDM2*, *TERT*, *CCND1*, *CCNE1*, and *NKX2-1* and deletions of *CDKN2A/B* and *PTEN* (12, 14–17). However, for many of these recurrently amplified regions, the target gene(s) believed to drive the pathogenesis of cancer remains to be identified and validated (12, 14–17). For example, chromosome 22q11.21 is focally amplified in 3% of lung adenocarcinoma samples and the peak region contains 15 genes, including *CRKL* (v-crk sarcoma virus CT10 oncogene homolog (avian)-like) (12, 16, 17). Recurrent amplifications of 22q11.21 have not been described in squamous cell lung carcinomas (18) or small cell lung carcinomas (19).

CRKL is an adaptor protein that participates in signal transduction in response to both extracellular and intracellular stimuli, such as growth factors, cytokines, and the oncogenic BCR-ABL fusion protein (20, 21). CRKL consists of an N-terminal Src homology 2 (SH2) domain followed by two SH3 domains (SH2-SH3N-SH3C) (20). The SH2 domain of CRKL binds to the phosphorylated Y-x-x-P motif present in many docking proteins, such as BCAR1 (also known as p130CAS), paxillin, and GAB (20, 21), whereas the SH3N domain binds to proline-rich P-x-x-P-x-K motif-containing proteins, such as Son of Sevenless (SOS), RAPGEF1 (also known as C3G) (22), p85 (23), ABL1, and BCR-ABL (24, 25). Through these interactions, CRKL facilitates the timely and localized formation of protein complexes required for signal transduction in many biological processes, including cell proliferation, survival, adhesion, and migration (20, 21).

CRKL and several proteins that interact with CRKL have been implicated in cancer. Overexpression of CRKL in Rat-1 fibroblast cells has been shown to promote anchorage-independent growth, but the signaling pathways necessary for this phenotype remain undefined (26, 27). Activating mutations of *ALK* have been shown to activate RAP1 through CRKL-C3G complexes in neuroblastomas (28). Moreover, expression of the oncogenic *RET-PTC1* fusion protein leads to increased RAP1 activity, whereas expression of a dominant interfering $RAP1^{N17}$ inhibits proliferation of papillary thyroid carcinoma cells (29). However, it remains unclear how overexpression of CRKL affects C3G-RAP1 signaling and whether RAP1 signaling plays a role in proliferation, survival, and transformation of NSCLC cells.

In previous work, we and others demonstrated that a subset of NSCLC is dependent on *CRKL* expression for proliferation (17, 30). Moreover, overexpression of CRKL in immortalized human lung epithelial cells promoted EGF-independent proliferation (17). Here we credential *CRKL* as an oncogene in NSCLC that transforms human lung epithelial cells through coordinate activation of the RAS and RAP1 pathways and is involved in resistance to EGFR inhibitors.

RESULTS

Amplification and Overexpression of the *CRKL* Gene in NSCLC Cells

In previous work, we and others found recurrent focal copy number gain at chromosome 22q11.21 involving *CRKL* in 3% of 371 primary lung adenocarcinomas, with another 13% of tumors exhibiting broad copy number gain spanning that region (12, 17). To identify other NSCLC cell lines that harbor copy number gain of this region, we examined a panel of 84 NSCLC cell lines that had been characterized by high-density single-nucleotide polymorphism arrays (19, 31) and identified 6 cell lines with high-level focal amplifications of 22q11.21 (Fig. 1A). We confirmed that *CRKL* was amplified by FISH in 3 of these cell lines: HCC515, H1819, and H1755 (Fig. 1B). In contrast, in the HCC1833 cell line in which we found normal 22q copy number (Fig. 1A), we detected only 2 copies of the *CRKL* gene (Fig. 1B). To confirm these findings, we also performed quantitative PCR to measure the copy number of *CRKL* and detected 12 to 18 copies of *CRKL* in NSCLC cell lines that harbored a 22q11.21 amplification (Fig. 1C).

To determine whether this observed gene amplification correlates with increased *CRKL* expression, we examined

Authors' Affiliations: Departments of [1]Medical Oncology and [2]Pediatric Oncology, [3]Lowe Center for Thoracic Oncology, and [4]Center for Cancer Genome Discovery, Dana-Farber Cancer Institute; [5]Massachusetts General Hospital Cancer Center; [6]Harvard Medical School; [7]Department of Pathology, Harvard Medical School; [8]Department of Medicine, Brigham and Women's Hospital, Harvard Medical School, Boston; and [9]Broad Institute of Harvard and MIT, Cambridge, Massachusetts

Note: Supplementary data for this article are available at Cancer Discovery Online (http://www.cancerdiscovery.aacrjournals.org).

Corresponding Author: William C. Hahn, Dana-Farber Cancer Institute, 450 Brookline Avenue, Dana 1538, Boston, MA 02115. Phone: 617-632-2641; Fax: 617-632-4005; E-mail: William_Hahn@dfci.harvard.edu

doi: 10.1158/2159-8290.CD-11-0046

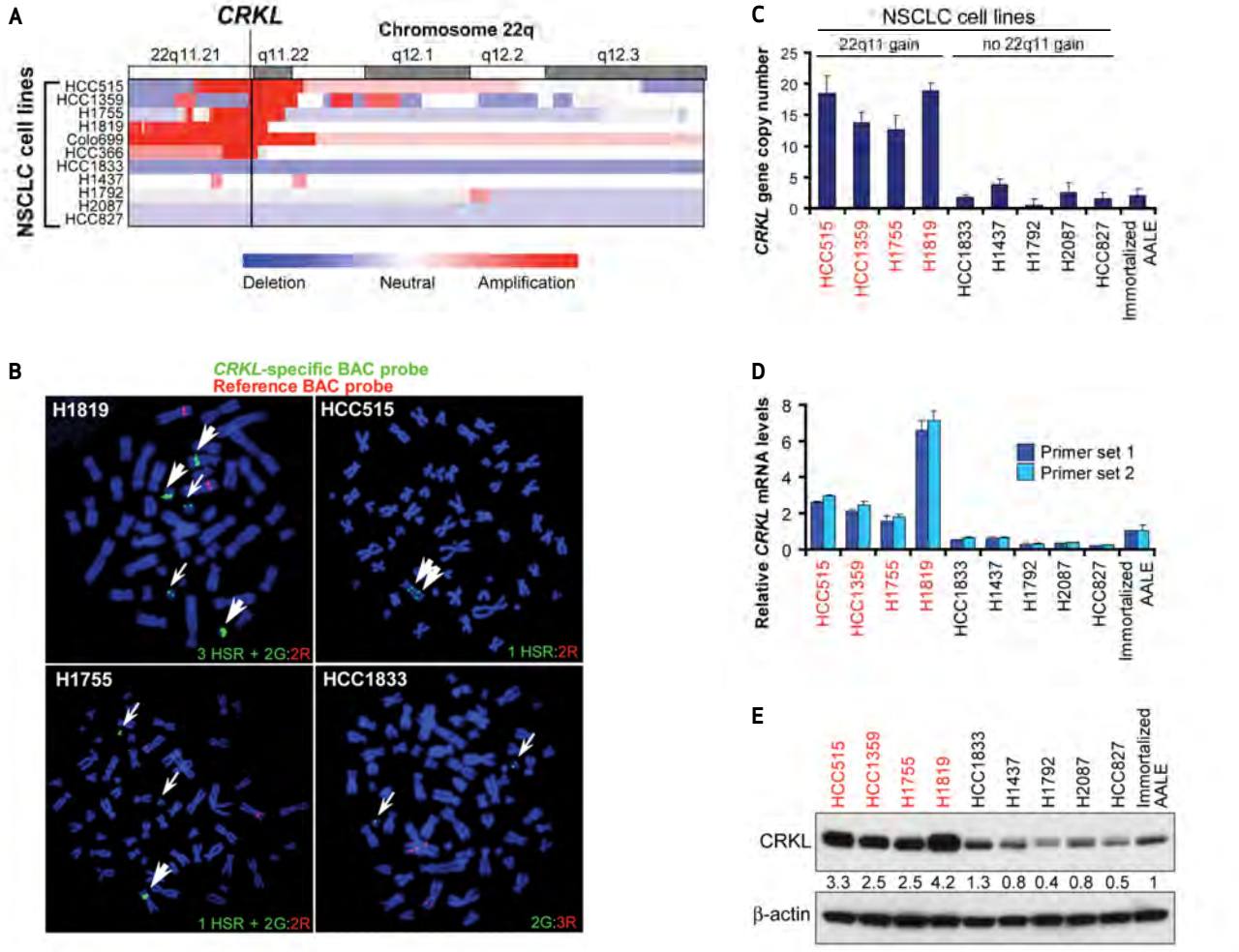

Figure 1. Amplification and overexpression of the *CRKL* gene in NSCLC cell lines with amplification of 22q11.21. **A,** single-nucleotide polymorphism array colorgram showing genomic amplification of chromosome 22q11.21 in NSCLC cell lines. Regions of genomic amplification and deletion are denoted in red and blue, respectively. **B,** FISH of NSCLC cells with the use of a *CRKL*-specific probe (green, G) and a reference probe (red, R). HSR, homogenously staining region. **C,** quantitative PCR analysis of *CRKL* copy number in NSCLC cells. *CRKL* copy number in NSCLC cells was normalized to *LINE-1* and immortalized AALE cells by use of the standard curve method. Data represent mean ± SD of triplicate measurements. **D,** quantitative RT-PCR analysis of *CRKL* mRNA levels in NSCLC cell lines and immortalized AALE cells. Data represent mean ± SD of triplicate measurements. **E,** immunoblot of CRKL in NSCLC cell lines and immortalized AALE cells. β-actin was used as a loading control. The relative intensity of CRKL levels is determined.

expression data from the same panel of NSCLC cell lines (31) and observed that each of the cell lines that harbored 22q11.21 amplification expressed high levels of *CRKL* (Supplementary Fig. S1). When using quantitative reverse-transcription PCR, we detected a 2- to 7-fold increase in *CRKL* mRNA levels in NSCLC cells that harbored a 22q11.21 amplification compared with immortalized but nontumorigenic human airway epithelial cells (AALE; Fig. 1D) (32). Correlating with these observed transcript levels, CRKL protein expression was also increased (2.5- to 4.2-fold increase) in NSCLC cells that harbored a 22q11.21 amplification (Fig. 1E and Supplementary Fig. S2A). We note that in addition to *CRKL*, 4 genes within the amplicon, *PI4KA*, *ZNF74*, *THAP7*, and *LZTR1*, were also expressed at greater levels in samples that harbored a 22q11.21 amplification (Supplementary Fig. S1). In addition, when we examined gene expression data, we found that *CRKL* was expressed at high levels in a subset of cell lines that lacked a 22q11.21 amplification (Supplementary Fig. S1C). We confirmed that CRKL protein expression was increased in these cell lines compared with AALE cells, suggesting that mechanisms other than gene amplification may also lead to CRKL overexpression. These observations confirm that *CRKL* is highly amplified and overexpressed in a subset of NSCLC cells.

NSCLC Cells That Harbor a 22q11.21 Amplification Are Dependent on *CRKL*

We and others showed that a subset of NSCLC is dependent on *CRKL* expression for proliferation (17, 30).

To examine whether NSCLC cells that harbor the 22q11.21 amplification require CRKL expression for cell proliferation or survival, we tested the effects of suppressing *CRKL* on the proliferation of several NSCLC cell lines and AALE cells. We found that *CRKL* suppression by 2 independent short hairpin RNAs (shRNAs) substantially decreased the proliferation of NSCLC cell lines with a 22q11.21 gain (HCC515, HCC1359, H1755, H1819, HCC366, and Colo699; Fig. 2A and Supplementary Fig. S2B) and that exhibited CRKL overexpression but not 22q11.21 gain (H1915, H2009, H28, and H1299; Supplementary Fig. S2A and B). In contrast, suppression of *CRKL* in 2 NSCLC cell lines (H1833 and H1792) that have normal copy number at 22q11.21 and express lower levels of CRKL were relatively insensitive to *CRKL* suppression ($P = 0.0001$ and $P = 0.0056$ for shCRKL#1 and shCRKL#2, respectively, compared with cell lines that harbored a 22q11.21 gain, *t* test; Fig. 2A). In addition, the proliferation of immortalized AALE cells, which also exhibit normal copy number at 22q11.21, was unaffected by *CRKL* suppression (Fig. 2A).

To confirm that the observed effects of these shRNAs on proliferation were specific for *CRKL*, we constructed a shRNA-resistant CRKL mutant ($CRKL^{silent\ mutant}$) that contained multiple nucleotide substitutions to the targeting sequence of shCRKL#1 that do not change the amino acid sequence of CRKL (Fig. 2B). We then tested whether expression of the $CRKL^{silent\ mutant}$ rescued the decreased proliferation induced by shCRKL#1 and 2 other shRNAs that target the 3′ untranslated region (3′UTR) of *CRKL* mRNA (shCRKL#2 and shCRKL#3). We found that expression of the $CRKL^{silent\ mutant}$ permitted H1755 cells expressing each of these *CRKL*-targeting shRNAs to proliferate, whereas the expression of a control vector failed to rescue such cells (Fig. 2B). These observations extend the findings of previous studies (17) and reveal that NSCLC cells that harbor amplifications of 22q11.21 are particularly dependent on *CRKL* expression for proliferation, suggesting that, like other oncogenes, amplification of *CRKL* induces oncogene addiction (33).

To determine whether *CRKL* suppression induced apoptosis, we performed immunoblotting for PARP and caspase-3. We found that suppression of *CRKL* in H1755 cells harboring 22q11.21 amplifications resulted in the cleavage of PARP and caspase-3 (Fig. 2C). In contrast, no cleaved forms of PARP and caspase-3 were detected after the suppression of CRKL in HCC1833 cells that did not harbor 22q11.21 gain. These findings show that suppression of *CRKL* induced apoptotic cell death in NSCLC cells with *CRKL* amplifications.

We next investigated which domains were essential for CRKL-induced oncogene addiction. Specifically, we generated CRKL mutants with amino acid substitutions predicted to disrupt the function of the SH3N domain (W160L), the SH3C domain (W275L), or Tyr207 phosphorylation (Y207F) (26). We then tested whether expression of these CRKL mutants rescued the decreased cell proliferation induced by *CRKL* suppression. We first introduced a control vector or each of these *CRKL* mutants into H1755 cells and then introduced a *CRKL*-specific shRNA (shCRKL#3) that targets the 3′UTR of *CRKL* mRNA (Supplementary Fig. S2C). We found that expression of exogenous wild-type CRKL, $CRKL^{Y207F}$, or $CRKL^{W275L}$ mutants permitted cells expressing the *CRKL*-specific shRNA to proliferate (Fig. 2D), whereas the expression of the SH3N mutants (either $CRKL^{W160L}$ or $CRKL^{W160L+Y207F}$) or a control vector failed to rescue such cells (Fig. 2D). These findings demonstrate that the SH3N domain is essential for CRKL function in NSCLC cell lines with increased 22q11.21 copy number.

Suppression of *CRKL* in NSCLC Cells Inhibits Tumor Growth

To examine whether *CRKL* suppression affected tumorigenic growth of NSCLC cells that harbor *CRKL* amplification, we confirmed that HCC515 cells were able to form tumors after subcutaneous implantation into immunodeficient mice. To enable noninvasive monitoring of tumor growth by luminescent imaging, we generated a polyclonal population of HCC515 cells stably expressing luciferase. We then introduced either a scrambled control shRNA or a validated *CRKL*-specific shRNA (shCRKL#1) in vectors in which the expression of shRNA was under the control of a doxycycline-inducible promoter. Doxycycline treatment of cells containing the inducible shRNA (shCRKL#1) induced decreased CRKL protein levels compared with cells grown in the absence of doxycycline (Fig. 3A).

In contrast, treatment with doxycycline did not affect CRKL protein levels in cells expressing the scrambled control shRNA. We then injected cells expressing the inducible control shRNA or the *CRKL*-specific shRNA subcutaneously into opposite flanks of the same immunodeficient mice and allowed tumors to form (65 mm^3 in volume, 11 days; Fig. 3B). After 3 weeks, we observed that in mice feeding on doxycycline-containing chow, tumors expressing the control shRNA grew large whereas tumors expressing the *CRKL*-specific shRNA exhibited growth arrest (Fig. 3C and D). As expected, mice fed with normal chow grew large tumors with comparable size under uninduced condition (Fig. 3C and D). To determine whether *CRKL* suppression induced apoptotic cell death in tumors, we performed terminal deoxynucleotidyl transferase–mediated dUTP nick end labeling (TUNEL) staining and detected a significantly increased percentage of TUNEL-positive cells in tumors expressing *CRKL*-specific shRNA compared with tumors expressing a control shRNA (Fig. 3E). Together, these findings demonstrate that *CRKL* is required for tumorigenic growth of NSCLC cells with *CRKL* amplifications.

Overexpression of CRKL in Immortalized Human Airway Epithelial Cells Induces Anchorage-Independent Colony Formation

Overexpression of CRKL promotes anchorage-independent growth of Rat-1 fibroblast cells (27) but not NIH3T3 cells (34), demonstrating that transformation induced by CRKL expression is context dependent. To dissect the mechanism and genetic context required for the transformation of NSCLC, we used human airway epithelial cells that can be rendered tumorigenic by the introduction

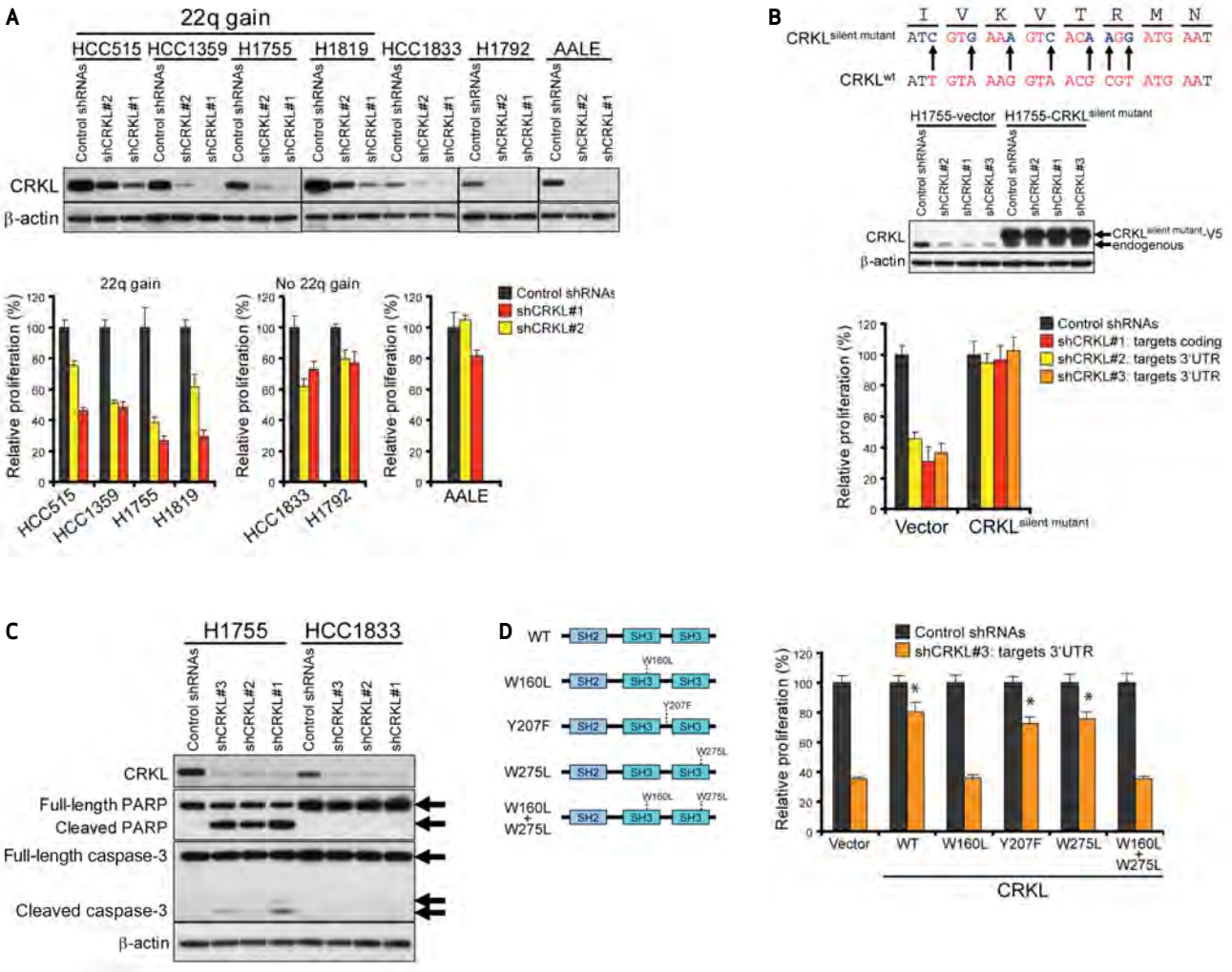

Figure 2. Suppression of *CRKL* decreases the proliferation of NSCLC cells harboring 22q11.21 amplifications. **A,** effect of *CRKL* suppression on relative proliferation of NSCLC cell lines and AALE cells. Top, immunoblot of CRKL proteins in each cell line expressing control shRNAs or 2 distinct *CRKL*-specific shRNAs. Bottom, cell proliferation 6 days after infection with the indicated shRNAs for each cell line. Data represent mean ± SD of 6 replicate measurements. **B,** effect of expression of shRNA-resistant CRKL on the proliferation of H1755 cells expressing *CRKL*-specific shRNAs. Top, generation of a shRNA-resistant CRKL cDNA (CRKL$^{silent\ mutant}$). The 21-mer sequence targeted by shCRKL#1 is marked in red. Middle, immunoblot of CRKL 4 days after infection with the indicated shRNAs in H1755 cells expressing a control vector or V5-epitope tagged CRKL$^{silent\ mutant}$. Bottom, effect of *CRKL* suppression by *CRKL*-targeting shRNAs on the proliferation of H1755 cells expressing a control vector or CRKL$^{silent\ mutant}$. shCRKL#2 and shCRKL#3 target the 3′UTR of endogenous *CRKL* mRNA. **C,** effect of *CRKL* suppression on cleavage of PARP and caspase-3 proteins in NSCLC cells. Immunoblots of PARP and caspase-3 proteins in H1755 and HCC1833 cells expressing the indicated shRNAs. **D,** effects of mutations on CRKL function in H1755 cells. Left, schematic of CRKL mutants. Right, effect of expressing wild-type or mutant CRKL on the proliferation of H1755 cells expressing a *CRKL*-specific shRNA (shCRKL#3). Data represent mean ± SD of 6 replicate measurements. *, $P < 0.0001$ as compared with cells expressing a control vector and shCRKL#3.

of specific combinations of genes (AALE cells) (32) to test whether CRKL expression induces cell transformation. Specifically, we introduced a retroviral vector encoding CRKL or a control vector into AALE cells and confirmed that CRKL was expressed at levels comparable with those found in NSCLC cells with *CRKL* amplification and overexpression (Fig. 4A). We found that overexpression of CRKL in AALE cells led to a >4-fold increase in anchorage-independent colony formation as compared with AALE cell lines expressing a control vector (Fig. 4B).

We also tested the ability of CRKL mutants that were predicted to disrupt the function of the SH3N domain (W160L), the SH3C domain (W275L), and Tyr207 phosphorylation (Y207F) to induce anchorage-independent growth. We found that the CRKL SH3C and Tyr207 mutants (W275L, Y207F, and Y207F+W275L) induced anchorage-independent colony formation similarly to wild-type CRKL when overexpressed in AALE cells (Fig. 4B). In contrast, the SH3N mutants (W160L, W160L+Y207F, and W160L+W275L) failed to promote anchorage-independent growth (Fig. 4B). These findings

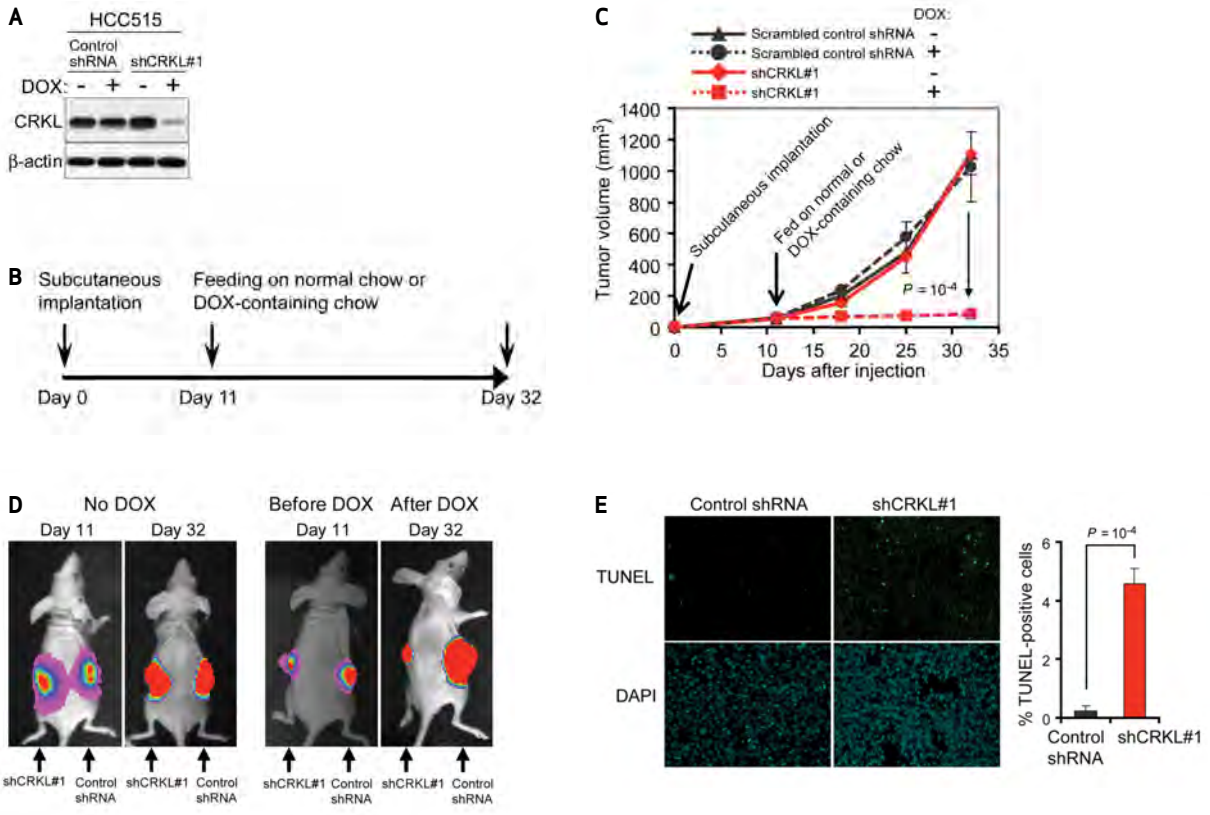

Figure 3. Effects of *CRKL* suppression on NSCLC tumorigenicity. **A,** generation of NSCLC cell lines expressing a doxycycline (DOX)-inducible *CRKL*-specific shRNA. A scrambled control shRNA or a validated CRKL-specific shRNA (shCRKL#1) under the control of DOX-inducible promoter were introduced into HCC515 cells. Immunoblot of CRKL proteins in cells in the absence or presence of 200 ng/mL DOX for 96 hours. **B,** experimental scheme. Each HCC515 cell line expressing a DOX-inducible vector encoding either shCRKL#1 or a scrambled control shRNA was implanted subcutaneously into opposite flanks of the same mouse ($n = 10$). Tumors were allowed to grow for 11 days to attain a volume of ∽65 mm^3. Mice were then fed on normal chow ($n = 5$) or DOX-containing chow ($n = 5$) to induce shRNA expression. Tumor growth was measured by caliper and bioluminescent imaging. **C,** effect of *CRKL* suppression on the growth of HCC515 xenografts. DOX-induced *CRKL* suppression induced growth arrest of tumors derived from cell lines as described in panels (A) and (B). Data represent mean ± SD. **D,** representative bioluminescent images of the growth of HCC515 xenografts. DOX-induced CRKL suppression induced growth arrest of tumors derived from cell lines as described in panels (A) and (B). Images shown are the day 11 images (before DOX) and day 32 images (with or without DOX). **E,** TUNEL staining of xenografts. Left, DOX-treated tumors expressing a control shRNA or shCRKL#1 were harvested on day 32 as described in (B) and stained for TUNEL (green) and DAPI (blue). Right, quantification of percent of TUNEL-positive cells. Mean ± SD are shown.

suggest that overexpression of CRKL in AALE cells induces cell transformation that is dependent on the integrity of the SH3N domain.

CRKL Induces Cell Transformation by Coordinately Activating Multiple Signaling Pathways

The SH3 domain of CRKL and other CRK family proteins interacts with many proline-rich motif-containing proteins, such as SOS, C3G (35, 36), and p85 (23), implicating CRKL in the regulation of several pathways including those regulated by RAS–mitogen-activated protein kinase (MAPK) (27, 37), C3G-RAP1 (38–42), and phosphoinositide 3-kinase (PI3K)-AKT (23, 43, 44). Thus, we hypothesized that overexpression of CRKL induces cell transformation through coordinate activation of several signaling pathways. To investigate the mechanism by which CRKL induces cell transformation in human NSCLC, we first determined whether overexpression of CRKL alters the phosphorylation state of tyrosine kinases in AALE cells. Specifically, we applied a multiplex method that uses Luminex beads precoupled with protein-specific or phospho-specific antibodies (Supplementary Fig. S3) to isolate the majority of tyrosine kinases and other kinases followed by measurement of tyrosine phosphorylation levels using a phospho-tyrosine-specific antibody (4G10) (45). We detected significantly increased levels of phospho-T185/Y187 ERK1/2 and phospho-Y419 SRC proteins in AALE cells expressing wild-type CRKL compared with cells transfected with a control vector

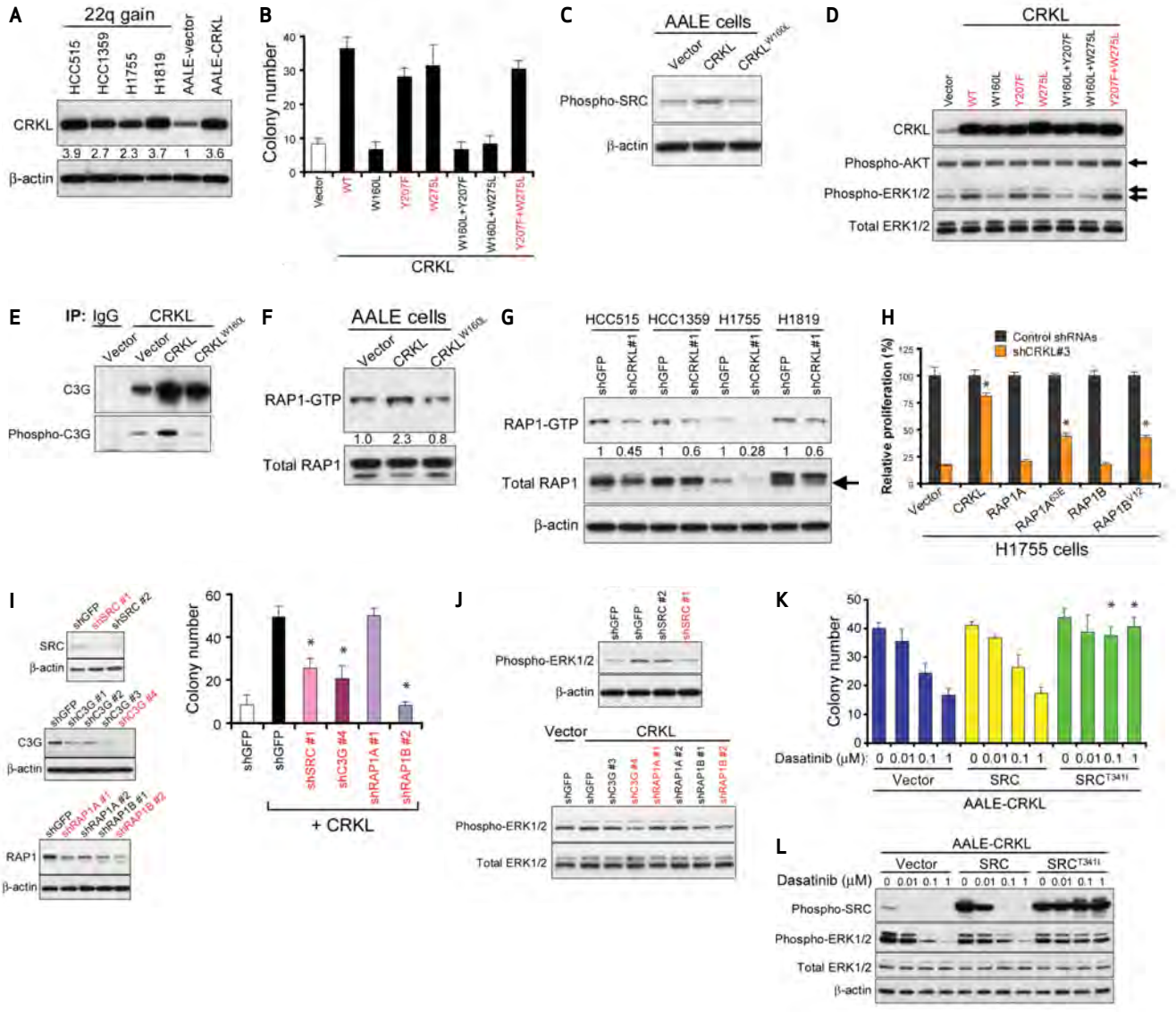

Figure 4. The role of SRC-C3G-RAP1 signaling in transformation induced by CRKL. **A,** immunoblot of CRKL in AALE cell lines overexpressing a control vector or CRKL compared with NSCLC cells with *CRKL* amplifications. The relative intensity of bands is determined. **B,** anchorage-independent growth of AALE cell lines stably overexpressing a control vector, wild-type (WT), or mutant CRKL. Colony number indicates colonies > 0.2 mm in diameter 4 weeks after plating. Data represent mean ± SD of 6 replicates from 2 independent experiments. Wild-type CRKL and CRKL mutants that induce anchorage-independent growth are marked in red. **C,** overexpression of CRKL in AALE cells increased the phosphorylation of SRC. Immunoblot of phospho-Y419 SRC proteins in AALE cells overexpressing a control vector, CRKL, or $CRKL^{W160L}$ mutant. **D,** immunoblot of phospho-T185/Y187 ERK1/2 and phospho-S473 AKT in AALE cell lines overexpressing wild-type (WT) or mutant CRKL. Wild-type CRKL and CRKL mutants that induced anchorage-independent growth in panel (B) are marked in red. **E,** effect of CRKL overexpression on the CRKL-C3G interaction and phosphorylation of C3G in AALE cells. CRKL immune complexes in AALE cells expressing indicated constructs were isolated and immunoblotting for phosphorylated C3G and total C3G protein was performed by the use of specific antibodies. **F,** overexpression of CRKL in AALE cells increased RAP1 activity. A pull-down assay for GTP-bound RAP1 proteins was performed followed by immunoblotting for RAP1 proteins. An immunoblot for RAP1 protein in total lysates before the pull-down assay was used as loading control. The relative intensity of bands is determined. **G,** effect of *CRKL* suppression on RAP1 activity in NSCLC cells that harbored amplification of *CRKL*. Pull-down assays were performed to assess the RAP1-GTP levels in NSCLC cells 4 days after infection with a control shRNA targeting *GFP* or a *CRKL*-specific shRNA (shCRKL*#*1) followed by immunoblotting for RAP1. An immunoblot of RAP1 proteins in total lysates shows the relative intensity of bands. Arrow indicates RAP1 protein. **H,** effect of expressing RAP1 on cell proliferation of H1755 cells after *CRKL* suppression. Each H1755 cell line expressing a control vector, wild-type RAP1A or RAP1B, or constitutively active $RAP1A^{63E}$ or $RAP1B^{V12}$ mutants was infected with control shRNAs or a *CRKL*-specific shRNA (shCRKL*#*3). Cell proliferation was measured 6 days after infection with shRNA. Data represent mean ± SD of 6 replicate measurements. *, $P < 0.0001$ as compared with cells expressing a control vector and shCRKL*#*3. **I,** effect of suppression of SRC, C3G, or RAP1 on CRKL-induced anchorage-independent growth. Left, immunoblots of SRC, C3G, or RAP1 proteins in CRKL-overexpressing AALE cells expressing a control shRNA targeting *GFP* or each gene-specific shRNA. The shRNAs that suppressed the target protein the best are marked in red. The antibody for RAP1 detects both RAP1A and RAP1B. Right, anchorage-independent growth of AALE cells expressing indicated constructs. Colony number indicates colonies >0.2 mm in diameter 4 weeks after plating. Data represent mean ± SD of 6 replicate determinations from 2 independent experiments. *, $P < 0.001$ as compared to cells expressing CRKL and shGFP. **J,** effect of suppression of SRC, C3G, or RAP1 on phospho-ERK1/2 levels in CRKL-overexpressing AALE cells. Immunoblots of phospho-ERK1/2 in CRKL-overexpressing AALE cells expressing the indicated shRNAs. The shRNAs marked in red were validated in panel (I). **K,** effect of dasatinib treatment on anchorage-independent growth of CRKL-overexpressing AALE cells that expressed wild-type SRC, mutant SRC, or a control vector in the presence of dasatinib at the indicated concentrations. The colony number indicates colonies >0.2 mm in diameter 4 weeks after plating. Mean ± SD are shown. *, $P < 0.001$ compared with cells expressing a control vector. **L,** effect of dasatinib treatment on phospho-SRC and phospho-ERK1/2 in CRKL-overexpressing AALE cells. AALE cells expressing the indicated constructs were exposed to dasatinib at the indicated concentrations for 6 hours followed by immunoblotting.

or the CRKL^{W160L} mutant that failed to induce cell transformation ($P = 0.0244$ and $P = 0.0035$, respectively, *t*-test; Supplementary Fig. S3).

We confirmed that AALE cells stably overexpressing CRKL exhibited increased levels of phospho-Y419 SRC (Fig. 4C) and phospho-T185/Y187 ERK1/2 (Fig. 4D) compared with cells expressing a control vector by immunoblotting with phospho-specific antibodies. Moreover, CRKL mutants (Y207F, W275L, and Y207F+W275L) that induced anchorage-independent growth when overexpressed in AALE cells also led to increased levels of phospho-ERK1/2, whereas CRKL mutants (W160L, W160L+Y207F, and W160L+W275L) that failed to induce anchorage-independent growth failed to induce similar patterns of tyrosine phosphorylation (Fig. 4D). In contrast, phospho-S473 AKT levels remained unchanged between cells overexpressing CRKL or a control vector (Fig. 4D). These observations indicate that overexpression of CRKL in AALE cells results in specific, constitutive activation of both SRC and ERK1/2 signaling.

We next investigated whether CRKL-induced SRC activation plays a role in transformation of AALE cells. CRKL and SRC have been shown to share many common substrates, such as p130CAS and paxillin. Overexpression of CRKL in AALE cells also resulted in increased phosphorylation levels of p130CAS and paxillin compared with cells expressing a control vector or CRKL^{W160L} mutants (Supplementary Fig. S4A). Moreover, suppression of *CRKL* resulted in reduced phosphorylation levels of SRC and p130CAS at varied levels in NSCLC cells that harbored *CRKL* amplifications (Supplementary Fig. S4B). These results suggest that overexpression of CRKL may represent a mechanism for aberrant SRC activation and signaling in NSCLC cells.

Recently, activating point mutations of *ALK* have been shown to activate RAP1 through CRKL-C3G complexes in neuroblastomas (28). C3G, a guanine nucleotide-exchange factor required for RAP1 activation, has been shown to form stable complexes with CRKL and other CRK family members (35, 36), and SRC has been implicated in activation of C3G-RAP1 through CRK family adaptors (46). We therefore investigated the role of RAP1 signaling in CRKL-induced transformation of AALE cells by determining whether overexpression of CRKL in AALE cells affected its interaction with C3G and the phosphorylation status of C3G. We isolated CRKL immune complexes from AALE cells overexpressing CRKL and detected increased C3G bound to CRKL and, to a lesser extent, the CRKL^{W160L} mutant compared with cells expressing a control vector (Fig. 4E). We noted that increased phosphorylation levels of C3G were detected only in CRKL immune complexes isolated from CRKL-overexpressing AALE cells by immunoblotting with a phospho-specific antibody (Fig. 4E). These observations suggest that overexpression of CRKL promotes its interaction with C3G and modulates C3G activity.

We next determined whether overexpression of CRKL in AALE cells also altered RAP1 activity by performing pull-down assays to assess the levels of GTP-bound RAP1. Overexpression of CRKL in AALE cells induced substantially increased levels of RAP1-GTP (2.3-fold increase) compared with cells expressing a control vector or CRKL^{W160L} mutant (Fig. 4F). In addition, we found that suppression of *CRKL* in NSCLC cell lines that harbor *CRKL* amplifications resulted in reduction of both RAP1-GTP and total RAP1 levels (Fig. 4G). Moreover, inhibition of SRC with dasatinib (0.1 μM) led to decreased RAP1-GTP levels in 3 NSCLC cell lines that harbored *CRKL* amplifications (Supplementary Fig. S4C). These findings indicate that CRKL regulates RAP1 activity in a SRC-dependent manner in *CRKL*-amplified NSCLC cells.

To examine whether CRKL-induced RAP1 activation is required for the proliferation of NSCLC cells with *CRKL* amplifications, we tested the ability of constitutively active RAP1 mutants to rescue cells from the cytotoxic effect of *CRKL* suppression. We transduced H1755 cells with a control lentiviral vector or lentiviral vectors expressing wild-type or constitutively active RAP1 mutants and then introduced a *CRKL*-specific shRNA (shCRKL#3). We found that overexpression of constitutively active forms of RAP1A or RAP1B partially reversed the antiproliferative effect of *CRKL* suppression (Fig. 4H). In contrast, expression of wild-type RAP1A, RAP1B, or a control vector failed to affect the decreased proliferation induced by *CRKL* suppression (Fig. 4H). These findings suggest that CRKL-induced RAP1 activation in part is required for proliferation and survival of NSCLC cells with *CRKL* amplification. The partial rescue conferred by active RAP1 also suggests that CRKL may activate additional signaling pathways not involving RAP1 that are required for proliferation and survival.

Because RAP1 has been shown to modulate ERK signaling in a cell context-dependent manner (39–41), we examined whether CRKL-induced ERK activation and cell transformation requires a signaling pathway involving SRC-C3G-RAP1. Specifically, we introduced *SRC*-, *C3G*-, or *RAP1A/B*-specific shRNAs into AALE cells overexpressing CRKL and then assessed anchorage-independent growth. We found that shRNAs specific for *SRC*, *C3G*, or *RAP1B*, but not *RAP1A*, substantially decreased the anchorage-independent growth of CRKL–over-expressing AALE cells (Fig. 4I and Supplementary Fig. S5A). Correlating with these observations, suppression of SRC, C3G, or RAP1B in CRKL-overexpressing AALE cells resulted in decreased levels of phospho-ERK1/2 compared with cells expressing a control shRNA targeting *GFP* (Fig. 4J).

In contrast, suppression of p130CAS, one of the substrate proteins of CRKL and SRC, failed to inhibit CRKL-induced ERK activation and anchorage-independent growth in AALE cells (Supplementary Fig. S4D). To confirm that SRC is required for CRKL-induced cell transformation, we assessed the anchorage-independent growth of AALE cells overexpressing CRKL in the presence of the SRC inhibitor dasatinib. SRC inhibition significantly decreased the anchorage-independent growth and phospho-ERK levels in CRKL-overexpressing AALE cells (Fig. 4K and L). Expression of the gatekeeper SRC^{T341I} mutant, but not wild-type SRC, conferred resistance to dasatinib and allowed CRKL-overexpressing AALE cells to grow in an anchorage-independent manner in the presence of dasatinib (Fig. 4K and L). Taken together, these findings suggest that the SRC-C3G-RAP1 signaling pathway is required for sustaining CRKL-induced ERK activation and cell transformation.

CRKL-Induced Cell Transformation Requires Activation of SOS1-RAS-RAF Signaling

Since prior work has linked CRKL function and RAS signaling (27, 37), we determined whether overexpression of CRKL in AALE cells altered RAS activity. We found that overexpression of CRKL in AALE cells resulted in increased levels of GTP-bound, active RAS (Fig. 5A). The CRKL-induced RAS activity in turn activates MAPK pathways as indicated by increased *in vitro* kinase activity of BRAF (Fig. 5B) and increased phosphorylation levels of RAF1 (Fig. 5C). These observations suggest that CRKL augments the activation of the RAS-RAF-MAPK pathway.

Previous investigators also have shown that CRK family proteins interact with SOS1, a guanine nucleotide-exchange factor that is a well-known RAS activator (22, 38, 47). We therefore determined whether overexpression of CRKL affects its interaction with SOS1 proteins in AALE cells. We isolated CRKL immune complexes and detected the presence of SOS1 proteins in AALE cells overexpressing CRKL but not in cells expressing a control vector or $CRKL^{W160L}$ mutant (Fig. 5D). The observation that CRKL promoted the interaction with SOS1 proteins via the SH3 domain suggests that overexpression of CRKL may recruit SOS1 proteins to the cell membrane and thereby facilitate RAS activation.

To examine whether CRKL-induced cell transformation requires activation of the RAS-RAF signaling pathway, we suppressed *SOS1*, *KRAS*, or different *RAF* members with RNAi in CRKL-overexpressing AALE cells and then evaluated anchorage-independent growth. Suppression of *SOS1*, *KRAS*, *BRAF*, or *RAF1*, but not *ARAF*, significantly inhibited the anchorage-independent growth of CRKL–over-expressing AALE cells (Fig. 5E and Supplementary Fig. S5B). These findings suggest that CRKL-induced cell transformation requires activation of SOS1-RAS-BRAF/RAF1 signaling pathways.

CRKL Cooperates with Loss of *NF1* to Induce Tumorigenicity in Human Lung Epithelial Cells

Expression of oncogenic alleles of H- or K-RAS confers the ability to form anchorage-independent colonies and tumors to AALE cells (Fig. 6A) (32). In contrast, overexpression of CRKL alone in AALE cells induced anchorage-independent growth but failed to allow tumor formation in AALE cells. In previous work, we and others found that the coexpression of activated alleles of members of known RAS effector pathways, such as mitogen-activated protein/extracellular signal–regulated kinase (MEK) and AKT or MEK and IKBKE, substitute for RAS and induce tumorigenicity (48–51). We therefore searched for potential candidates that would cooperate with CRKL to promote tumorigenicity in the context of lung epithelial cells.

We introduced constitutively active alleles or shRNAs into AALE cells that activated receptor tyrosine kinase signaling ($EGFR^{L858R}$), MAPK signaling ($BRAF^{V600E}$), PI3K-AKT signaling (myristoylated AKT1, $PIK3CA^{H1047R}$, or *PTEN*-shRNA), c-MYC, or RAS signaling (*NF1*-shRNA). We then introduced CRKL or a control vector into these cell lines and tested their ability to grow in anchorage-independent manner. We observed that overexpression of CRKL in combination with each of these alleles promoted anchorage-independent growth beyond that induced by CRKL alone (Fig. 6A). In particular, overexpression of CRKL together with *NF1* suppression showed a pronounced synergy in promotion of anchorage-independent growth ($P = 0.0006$ and $P = 0.0003$ compared with cells overexpressing *CRKL*- or *NF1*-shRNA alone, respectively, *t*-test; Fig. 6A). These results suggest that overexpression of CRKL promotes anchorage-independent growth in many different contexts.

Because coexpression of CRKL and $EGFR^{L858R}$, $BRAF^{V600E}$, or *NF1*-shRNA led to the most significant increase in anchorage-independent growth among all combinations tested, we examined whether overexpression of CRKL together with these alleles promotes tumorigenicity in immunodeficient mice. We found that the AALE cells overexpressing $EGFR^{L858R}$ or $BRAF^{V600E}$ were tumorigenic (Fig. 6B), suggesting that activation of EGFR or MAPK signaling suffice to induce tumorigenicity. Overexpression of CRKL in the setting of *EGFR* or *BRAF* expression failed to increase the rate of tumor formation. Interestingly, shRNA-mediated suppression of *NF1* in AALE cells failed to induce subcutaneous tumors in immunodeficient mice (Fig. 6B). In contrast, overexpression of CRKL together with *NF1* suppression conferred the ability to form tumors in 4 of 12 injection sites (33%) in AALE cells ($P = 0.006$, the Fisher exact test; Fig. 6B).

In consonance with these findings, the RAS-GTP levels (Fig. 6C) and *in vitro* BRAF kinase activity (Fig. 5B) were found to be highly increased in AALE cells coexpressing CRKL and *NF1*-shRNA, indicating a robust activation of RAS-RAF signaling. These observations further demonstrate the transforming capability of CRKL overexpression, which participates in promoting tumor formation in a context-dependent manner.

To investigate whether *CRKL* amplification and *NF1* loss co-occur in primary NSCLC tumors and cell lines, we reanalyzed mutation and copy number data generated in the Tumor Sequencing Project (12, 52). Among 188 primary lung adenocarcinomas, 1 of the 3 samples harboring focal amplification of *CRKL* was found to also harbor an inactivating mutation of *NF1*. No mutations were detected in the other oncogenes that were analyzed by sequencing in the remaining 2 CRKL-amplified tumor samples. In cell lines, we examined the expression of NF1 protein in 4 CRKL-amplified cell lines and found that HCC1359 cells failed to express NF1 compared with immortalized AALE cells (data not shown). These observations suggest that CRKL amplification and NF1 loss co-occur in a subset of NSCLCs and thus may cooperate in cell transformation.

Overexpression of CRKL Decreases Sensitivity of NSCLC to EGFR Inhibitor Treatment

We noticed mutual exclusivity between amplifications of *CRKL* and amplifications and mutations of *EGFR* in the 371 primary lung adenocarcinomas (Supplementary Fig. S6A) (12, 52). Specifically, we found that tumors with focal high-level *CRKL* amplifications did not exhibit amplifications of the *EGFR* gene ($P < 0.0001$, Fisher exact test; Supplementary Fig. S6A). Similarly, when we analyzed a panel of NSCLC cell lines (31, 53) by co-occurrence of genome alterations, we observed that the 6 *CRKL*-amplified cell lines appeared to form a subgroup distinct from the 12 cell lines with mutations

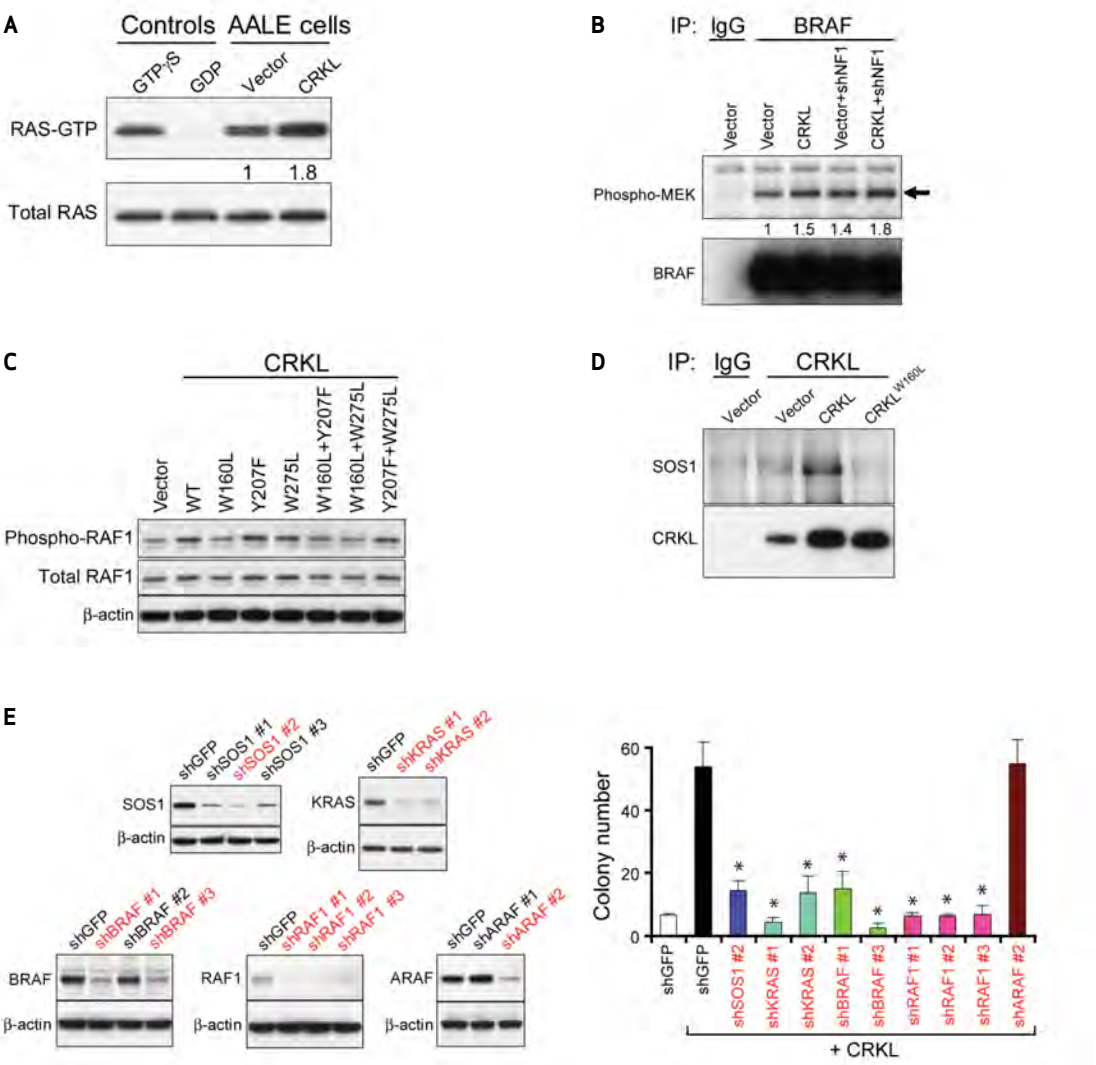

Figure 5. CRKL-induced cell transformation requires SOS1-RAS-RAF. **A,** overexpression of CRKL increased RAS activity. The levels of GTP-bound RAS in AALE cells overexpressing a control vector or CRKL were measured by a pull-down assay followed by immunoblotting for RAS. Total RAS levels in total lysates were used as loading control. Positive and negative technical controls were obtained by incubating the total lysates with a nonhydrolyzable analog of GTP (GTPγS) or GDP, respectively, before pull-down assays. **B,** overexpression of CRKL increased *in vitro* BRAF kinase activity. The BRAF proteins in AALE cells expressing the indicated constructs were isolated by immunoprecipitation. The kinase activity was assessed by incubation with substrate proteins (MEK1). Immunoblots of phospho-MEK1 and BRAF proteins in the isolated BRAF immune complexes after kinase activity assay are shown. Arrow indicates phospho-MEK protein. **C,** immunoblot of phospho-S338–RAF1 in AALE cell lines overexpressing wild-type or mutant CRKL. **D,** interaction between CRKL and SOS1 in AALE cells overexpressing CRKL. CRKL immune complexes were isolated followed by immunoblotting for SOS1 or CRKL proteins in AALE cells expressing the indicated constructs. **E,** CRKL-induced anchorage-independent growth requires SOS1-RAS-BRAF/RAF1 signaling. Left, immunoblots of SOS1, KRAS, BRAF, RAF1, or ARAF proteins in CRKL-overexpressing AALE cell lines expressing a control shRNA targeting *GFP* or each gene-specific shRNA. shRNAs that suppressed more than 50% of target protein levels are marked in red. Right, anchorage-independent growth of AALE cells expressing the indicated constructs. The colony number indicates colonies >0.2 mm in diameter 4 weeks after plating. Data represent mean ± SD of 6 replicates from 2 independent experiments. *, $P < 0.0001$ as compared with cells expressing CRKL and shGFP.

and/or high-level amplifications of *EGFR* ($P < 0.0001$, Fisher exact test; Supplementary Fig. S6B). These observations suggest that amplifications of *CRKL* and *EGFR* may share some proliferation/survival pathways.

To investigate whether CRKL overexpression promoted the proliferation and survival of NSCLC cells in response to EGFR inhibition, we determined whether overexpression of CRKL in a gefitinib-sensitive cell line (HCC827) exhibiting the $EGFR^{E746\text{-}A750del}$ mutation (54) but a normal copy number of 22q21.22 (Fig. 1A) and low expression levels of CRKL (Fig. 1C) affected gefitinib sensitivity. We observed that HCC827 cells overexpressing CRKL became resistant to gefitinib (IC_{50} = 2.2 μM) compared with cells expressing a control vector (IC_{50} = 0.01 μM; Fig. 7A).

We next examined whether CRKL-induced ERK and SRC activation observed in the transformation of AALE cells

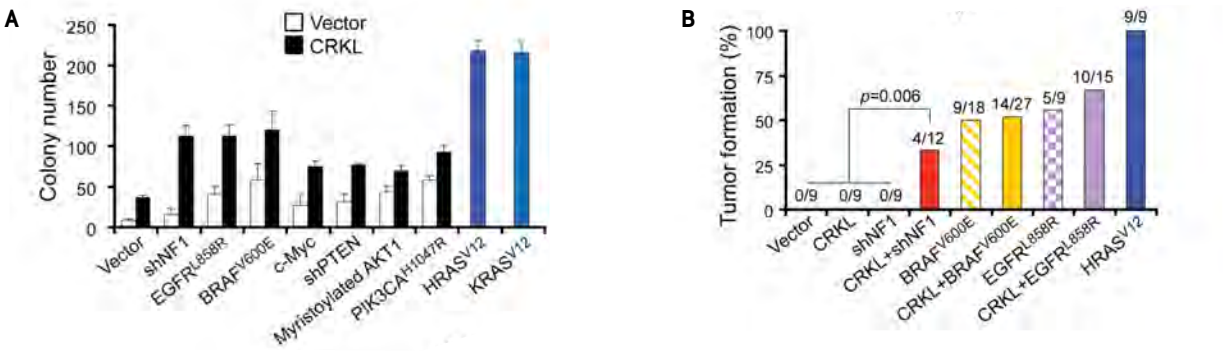

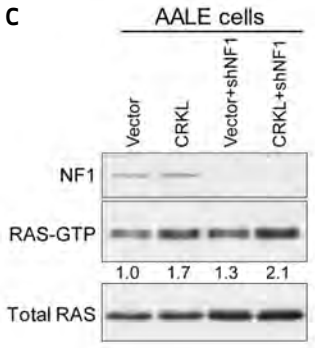

Figure 6. Overexpression of CRKL promotes tumor formation. **A,** overexpression of CRKL promotes anchorage-independent growth of AALE cells. Anchorage-independent growth of AALE cell lines stably expressing the indicated constructs is shown. The colony number indicates colonies >0.2 mm in diameter 4 weeks after plating. Data represent mean ± SD of 6 replicates from 2 independent experiments. **B,** overexpression of CRKL cooperated with *NF1* suppression in inducing tumor formation by AALE cells. AALE cell lines expressing the indicated constructs were implanted subcutaneously into immunodeficient mice (2×10^6 cells per injection site). The frequency of tumor formation and the number of tumors formed/number of injections within 5 months after implantation are depicted. **C,** pull-down assay to determine RAS-GTP levels. AALE cell lines expressing the indicated constructs were subjected to a pull-down assay for RAS-GTP levels followed by immunoblotting for RAS. The relative intensity of RAS-GTP levels was determined. An immunoblot of RAS protein in the total lysates was used as loading control. An immunoblot of NF1 proteins is also shown.

were involved in EGFR inhibitor resistance in HCC827 cells induced by CRKL overexpression. We observed that, upon gefitinib treatment, the phosphorylation of EGFR was completely suppressed in HCC827 cells either overexpressing CRKL or a control vector (Fig. 7B). In contrast, phosphorylation of ERK1/2 persisted at substantially greater levels in the presence of gefitinib in HCC827 cells overexpressing CRKL compared with cells expressing a control vector (Fig. 7B). Overexpression of CRKL in HCC827 cells also markedly elevated phosphorylation levels of SRC compared with control vector-expressing cells that were unaffected by gefitinib (Fig. 7B). These results demonstrate that overexpression of CRKL in HCC827 cells activates persistent ERK and SRC signaling upon gefitinib treatment.

To determine whether SRC activation contributes to CRKL-induced EGFR inhibitor resistance, we examined whether SRC inhibition suppressed growth of CRKL-overexpressing HCC827 cells. Cells were exposed to dasatinib alone or in combination with gefitinib. Interestingly, we observed that cells overexpressing CRKL also exhibited resistance to dasatinib treatment alone compared to cells expressing a control vector (Supplementary Fig. S7A). In addition, combined treatment failed to decrease the relative proliferation of CRKL-overexpressing cells compared with gefitinib treatment alone (Supplementary Fig. S7B and S7C). Moreover, activation of SRC or RAP1 by overexpression of SRC or constitutively active RAP1 alleles in HCC827 cells failed to induce resistance to gefitinib (Supplementary Fig. S8). Together, these results suggest that SRC activation is not required for CRKL-induced gefitinib resistance.

To investigate whether overexpression of CRKL affects its interaction with SOS1, we isolated CRKL immune complexes from HCC827 cells treated with or without an EGFR inhibitor and examined SOS1 interactions. We detected an increase in the abundance of SOS1 associated with CRKL in HCC827 cells overexpressing CRKL (Fig. 7C), and this interaction was further increased upon gefitinib treatment. These results suggest that overexpression of CRKL activates MAPK pathways by interacting with SOS1 in response to gefitinib.

To determine whether SOS1 was required for CRKL-induced EGFR inhibitor resistance, we introduced two SOS1-specific shRNAs or a control shRNA into CRKL-overexpressing HCC827 cells and measured the gefitinib sensitivity. Although suppression of SOS1 alone led to a reduction in proliferation (Supplementary Fig. S9A), suppression of SOS1 in combination with gefitinib resulted in a significant reduction in the relative proliferation of CRKL-overexpressing cells compared with cells treated with gefitinib alone (Fig. 7D). In contrast, expression of the control shRNA targeting *GFP* failed to alter gefitinib

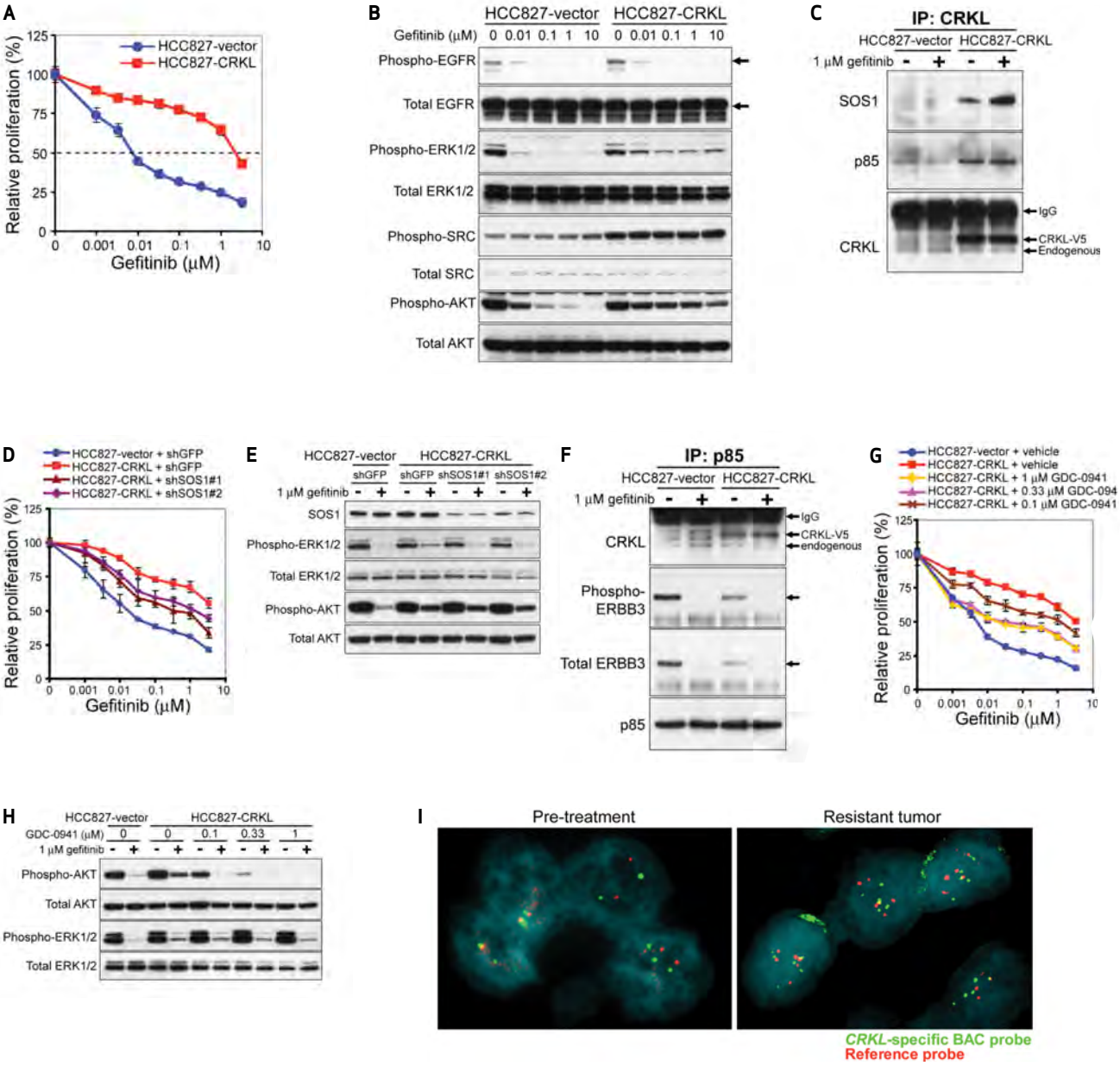

Figure 7. Overexpression of CRKL induces EGFR inhibitor resistance in NSCLC cells with *EGFR* mutations. **A,** effect of overexpressing CRKL on gefitinib sensitivity in HCC827 cells harboring an *EGFR* mutation. Cell proliferation was measured 72 hours after treatment with gefitinib. Data represent mean ± SD of triplicate measurements relative to untreated cells. **B,** effect of overexpressing CRKL on phosphorylation levels of EGFR, ERK, AKT, and SRC in response to gefitinib. HCC827 cells expressing a control vector or CRKL were exposed to gefitinib at the indicated concentrations for 6 hours and cell lysates were collected for immunoblotting with the indicated specific antibodies. **C,** effect of overexpressing CRKL on its interaction with SOS1 proteins. HCC827 cells expressing a control vector or CRKL were exposed to 1 μM gefitinib for 6 hours. After isolating CRKL immune complexes from cell extracts, immunoblotting for SOS1 and CRKL proteins was performed. **D,** effect of SOS1 suppression on CRKL-induced gefitinib resistance. Cell proliferation of each HCC827 cell line expressing the indicated constructs was measured 3 days after treatment with gefitinib. Data represent mean ± SD of 6 replicate determinations relative to untreated cells for each cell line. **E,** effect of SOS1 suppression on phospho-ERK levels in CRKL-expressing HCC827 cells in response to gefitinib. Cells expressing the indicated constructs were exposed to 1 μM gefitinib for 6 hours followed by immunoblotting with the indicated specific antibodies. **F,** effect of overexpressing CRKL on the interaction of p85 with CRKL and ERBB3 proteins. HCC827 cells expressing a control vector or CRKL were either untreated or treated with 1 μM gefitinib for 6 hours. After isolating p85 immune complexes, immunoblotting for CRKL, phospho-Y1289 ERBB3, total ERBB3, and p85 proteins was performed. **G,** effect of GDC-0941 on CRKL-induced gefitinib resistance. Cell proliferation of CRKL-expressing HCC827 cells was measured 3 days after treatment with gefitinib alone or in combination with GDC-0941 at the indicated concentrations. Data represent mean ± SD of triplicate measurements. **H,** effect of GDC-0941 on phospho-AKT levels in CRKL-expressing HCC827 cells in response to gefitinib. Cells were exposed to 1 μM gefitinib alone or in combination with GDC-0941 at indicated concentrations for 6 hours followed by immunoblotting with specific antibodies. **I,** acquired amplification of *CRKL* in an EGFR inhibitor-resistant lung tumor. FISH analysis of a NSCLC obtained from a patient prior to EGFR inhibitor therapy (left) or after acquiring drug resistance (right) using a *CRKL*-specific probe (green) and chromosome 22 telomere-specific probe (red) was performed. Nuclei were stained with DAPI (blue).

resistance (Fig. 7E). In consonance with these observations, suppression of SOS1 in CRKL-overexpressing HCC827 cells led to reduced phospho-ERK1/2 levels compared with cells expressing shGFP upon treatment with gefitinib (Fig. 7E). These results suggest that SOS1-dependent MAPK signaling contributes in part to CRKL-induced gefitinib resistance.

Because *MET* amplification has been shown to induce gefitinib resistance in *EGFR*-mutant tumors by activating ERBB3-dependent PI3K-AKT signaling (54), we examined whether overexpression of CRKL in HCC827 cells affects phosphorylation of AKT in response to gefitinib. We observed that, upon treatment with gefitinib, phosphorylation of AKT persisted at substantially greater levels in HCC827 cells overexpressing CRKL compared with cells expressing a control vector (Fig. 7B). These results suggest that like MET, overexpression of CRKL in HCC827 cells leads to persistent AKT signaling in response to gefitinib.

Since CRKL has been shown to interact with the p85 regulatory subunit of PI3K (23), we hypothesized that overexpression of CRKL promotes its interaction with p85 proteins to induce persistent PI3K/AKT signaling that is resistant to gefitinib treatment. We isolated CRKL immune complexes from HCC827 cells that overexpressed CRKL or a control vector and detected a markedly increased interaction with p85 proteins in cells over-expressing CRKL (Fig. 7C). Consistently, when we isolated endogenous p85 immune complexes, we also detected increased interaction between p85 and CRKL proteins in cells that overexpressed CRKL (Fig. 7F). Treatment with gefitinib did not affect this enhanced interaction between CRKL and p85 proteins (Fig. 7C and F). In contrast, overexpression of CRKL in HCC827 cells reduced the interaction between p85 and phospho-ERBB3 or ERBB3 proteins under normal culture conditions (Fig. 7F). Upon treatment with gefitinib, the interaction between p85 and ERBB3 was completely disrupted in cells that either overexpressed CRKL or a control vector (Fig. 7F). Together, these results suggest that overexpression of CRKL promotes its interaction with p85 proteins to induce persistent ERBB3-independent PI3K/AKT signaling in the presence of an EGFR inhibitor.

To determine whether CRKL-induced EGFR inhibitor resistance involves PI3K/AKT activation, we examined whether treatment with the PI3K inhibitor GDC-0941 suppressed growth of CRKL-overexpressing HCC827 cells in response to gefitinib. Cells were exposed to GDC-0941 alone or in combination with gefitinib. Combined treatment with GDC-0941 and gefitinib resulted in a substantial decrease in the relative proliferation of CRKL-overexpressing HCC827 cells compared with gefitinib treatment alone (Fig. 7G). The observed decrease in proliferation correlates with decreased phosphorylation levels of AKT in CRKL-overexpressing HCC827 cells after combined treatment with GDC-0941 and gefitinib (Fig. 7H). Similar findings were also observed with another PI3K inhibitor, LY294002 (Supplementary Fig. S9B–D). In contrast, combined treatment with the MET inhibitor PHA665752 and gefitinib failed to alter the relative proliferation of CRKL-overexpressing HCC827 cells (Supplementary Fig. S9E). These observations show that activation of PI3K-AKT signaling contributes to CRKL-induced EGFR inhibitor resistance.

CRKL Amplification in EGFR Inhibitor-Resistant Lung Cancer

We next examined whether amplification of *CRKL* occurs in *EGFR*-mutant tumors that develop acquired resistance after EGFR inhibitor treatment by performing FISH on 11 EGFR inhibitor-resistant tumors. We identified copy number gain of *CRKL* (with an average of 5.7 ± 0.3 copies per cell; Fig. 7I) in one EGFR inhibitor-resistant sample that was not present in the sample obtained before EGFR inhibitor treatment (average of 2.2 ± 0.2 copies of *CRKL* per cell). Since we also detected increased signal by using a chromosome 22 telomere-specific probe (5.7 ± 0.3 copies per cell), we concluded that the amplification event likely involves the gain of a large fraction of chromosome 22. This patient had shown a prolonged response to erlotinib for 2 years but showed signs of tumor regrowth while still receiving the treatment.

Although 8 of 11 tumors had acquired the known resistance-inducing *EGFR* T790M mutation, several laboratories have reported that other known resistance mechanisms may occur concomitantly with the *EGFR* T790M mutation, including *MET* amplification (54) and *CTNNB1* (β-catenin) mutations (55). These observations indicate that the copy number gain of *CRKL* detected in the EGFR inhibitor-resistant tumor represents a new genetic event after treatment and implicates amplification of *CRKL* as a mechanism of acquired resistance to EGFR inhibitor treatment in a subset of NSCLCs.

DISCUSSION

Amplification of *CRKL* Defines a New Subset of NSCLCs

In previous work, we and others identified a recurrent high-level and focal amplification peak on chromosome 22q11.21 in 3% of primary lung adenocarcinomas ($n = 371$) (12). An additional 13% of tumors exhibited broad copy number gain spanning that region (12, 17). We also observed a mutually exclusive relationship between amplification of *CRKL* and *EGFR* in both primary lung adenocarcinomas and the DFCI-84 NSCLC cell line collection. Herein, we extend previous work that showed that proliferation of NSCLC cells harboring a 22q11.21 amplification containing the *CRKL* gene depends on CRKL expression to a larger panel of NSCLC cell lines and show that suppression of *CRKL* induces apoptosis. Suppression of *CRKL* in established tumors derived from NSCLC cells with amplification of *CRKL* induced tumor regression *in vivo*. Overexpression of CRKL in immortalized human airway epithelial cells induced anchorage-independent growth and cooperated with suppression of *NF1* to induce tumorigenicity *in vivo*. Furthermore, we demonstrated that amplification of *CRKL* and loss of *NF1* co-occur in a subset of NSCLC. These observations implicate *CRKL* as a NSCLC oncogene. Although *CRKL* amplifications occur in a relatively small fraction of NSCLC, the finding that a similar fraction of NSCLC with translocations involving *ALK* respond to

treatment with crizotinib indicates that targeting genetic alterations present even in a subset of NSCLC may have clinical importance.

Amplification of *CRKL* Induces Cell Transformation by Activating RAS and RAP1 Signaling

By using both biochemical and genetic approaches, we have found that malignant transformation induced by CRKL involves both RAS and RAP signaling. By using a multiplex Luminex assay, we identified ERK and SRC as the downstream targets of CRKL. We further confirmed that CRKL activates RAS-RAF-ERK and SRC-RAP1 signaling by forming complexes with SOS1 and C3G, respectively. Our findings that expression of constitutively active RAP1 partially rescued NSCLC cells from proliferation inhibition induced by *CRKL* suppression define an important role of RAP1 signaling in proliferation and survival of NSCLCs with *CRKL* amplifications.

In a previous report in which the authors used a cell-free assay system, they showed that recombinant RAP1 stimulates BRAF kinase activity at a comparable level to KRAS (42). RAP1 was also able to enhance KRAS-stimulated BRAF kinase activity in an additive manner (42). In agreement with these findings, we found that RAP1 activation contributes to CRKL-induced MAPK activation and anchorage-independent growth in AALE cells. These findings suggest that CRKL induces transformation of human airway epithelial cells through its ability to coordinate activation of both RAS and RAP1 pathways, resulting in robust activation of MAPK signaling.

Overexpression of *CRKL* Induces Resistance to Small-Molecule EGFR Inhibitors

Although most NSCLCs with *EGFR* mutations initially respond to treatment with an EGFR inhibitor, the majority of these tumors ultimately develop resistance to the treatment. In approximately one-half of these cases, resistance is attributable to the occurrence of a secondary mutation (T790M) in *EGFR*. Prior study showed that other genetic events, such as amplification of *MET* or mutation of *PIK3CA*, may contribute to drug resistance in some of the remaining cases and also co-occur with secondary *EGFR* mutations, possibly because of the selection of drug-resistant clones using different resistance mechanisms (54, 55). These alterations promote cell growth by activating PI3K-AKT signaling in the presence of an EGFR inhibitor. Here we report that overexpression of CRKL in *EGFR*-mutant cells induces resistance to an EGFR inhibitor by activating both SOS1-dependent MAPK and p85-dependent PI3K-AKT signaling.

When we examined samples derived from tumors resistant to EGFR inhibitor treatment, we found *CRKL* amplifications in a patient whose tumors exhibited a clinical response to EGFR inhibitor therapy but subsequently developed acquired resistance. Because *CRKL* amplification was not identified in a pretreatment sample, these observations implicate *CRKL* amplifications as another mechanism of resistance to EGFR inhibitor therapy beyond secondary EGFR mutations, *MET* amplifications, and *PIK3CA* mutations (55).

CRKL as a Novel Therapeutic Target in NSCLCs Harboring *CRKL* Amplifications

We found that suppression of *CRKL* has no effect on proliferation of AALE cells but selectively induced apoptotic cell death in NSCLC cells with *CRKL* amplifications, suggesting that targeting CRKL may have a high therapeutic index. By using both RNAi and a complementation approach, we further confirmed that disruption of the SH3N domain abolished the ability of CRKL to rescue NSCLC cells from shCRKL-induced apoptosis. Our findings not only validate CRKL as a therapeutic target but also demonstrate that blocking the function of the SH3N domain is sufficient to modulate CRKL activity in NSCLCs harboring *CRKL* amplifications.

The statistical analysis of copy number alterations in 3,131 cancer specimens derived from 27 histologic types identified the 22q11.21 amplicon as one of the top 12 most commonly amplified regions in multiple cancer types (GISTIC q-value $= 3.71 \times 10^{-26}$), including NSCLCs, melanoma, ovarian, and colorectal cancers (19). *CRKL* is located at the center of the minimal region of amplification at 22q11.21 (19). These findings suggest that *CRKL* acts as an oncogene in other cancers harboring *CRKL* amplifications and that strategies to inhibit CRKL signaling may be useful in several cancer types.

METHODS

Plasmids

Human *CRKL* (obtained from the CCSB ORFeome collection) was cloned into pWzl-blast and pLenti6.3-blast-C-terminal V5 epitope-tagged vectors. The CRKL mutants ($CRKL^{W160L}$, $CRKL^{Y207F}$, $CRKL^{W275L}$, $CRKL^{W160L+Y207F}$, $CRKL^{W160L+W275L}$, $CRKL^{Y207F+W275L}$, $CRKL^{silent\ mutant}$) were generated by use of the Quikchange Site-Directed Mutagenesis kit (Stratagene). Human RAP1A, $RAP1A^{Q63E}$ (provided by Gromoslaw Smolen, Massachusetts General Hospital), RAP1B (Origene), and $RAP1B^{G12V}$ were cloned into the *Bam*HI and *Bsr*GI sites of pLenti6.3-blast. pLenti6.3-blast-SRC and SRC^{T351I} have been described (45). The pLenti6.2-blast-LacZ control vector was provided by Guo Wei, Dana-Farber Cancer Institute. pMKO.1-puro-shNF1, pBabe-puro-$HRAS^{V12}$, $KRAS^{V12}$, and myristoylated AKT1 have been described (51). pLKO.1-puro-shRNA constructs were obtained from The RNAi Consortium. The sequences targeted by *CRKL*-specific shRNAs are as follows: shCRKL#1 (TRCN0000006378), 5′-GCTCTGCTCTACCATGTTTAA-3′; shCRKL#2 (TRCN0000006380) 5′-CGTGAAAGTCACAAGGATGAA-3′; shCRKL#3 (TRCC0007470203), and 5′-GCCTACTGAGTAGCTTTCATT-3′. A pool of 85 control shRNAs targeting reporter genes (GFP, RFP, Luciferase, and LacZ) was used to generate control lentiviruses (Control shRNAs) (30). The sequences targeted by shGFP or scrambled control shRNA are 5′-ACAACAGCCACAACGTCTATA-3′ (TRCN0000072181) and 5′-GTGGACTCTTGAAAGTACTAT-3′, respectively. Other shRNA constructs used are as follows: shARAF#1 (TRCN0000000570), shARAF#2 (TRCN0000000567), shBCAR1#1 (TRCN0000115983), shBCAR#2 (TRCN0000115984), shBRAF#1 (TRCN0000006289), shBRAF#2 (TRCN0000006290), shBRAF#3 (TRCN0000006292), shRAF1#1 (TRCN0000001066), shRAF1#2 (TRCN0000001068), shRAF1#3 (TRCN0000001065), shKRAS#1 (TRCN0000033263), shKRAS#2 (TRCN0000003326), shRAP1A#1 (TRCN0000029784), shRAP1A#2 (TRCN0000029787), shRAP1B#1 (TRCN0000029176), shRAP1B#2 (TRCN0000029177), shSOS1#1 (TRCN0000048145), shSOS#2 (TRCN0000048144), shSOS1#3 (TRCN0000048146), shSRC#1 (TRCN0000195339), shSRC#2 (TRCN0000038150), shC3G#1 (TRCN0000048128), shC3G#2 (TRCN0000048129), shC3G#3 (TRCN0000048130), and shC3G#4 (TRCN0000048131).

Cell Culture and Virus Production

HCC515, H1819, HCC1833, H2087, and HCC827 cells were maintained in DMEM (Mediatech) supplemented with 10% FBS (Sigma-Aldrich). HCC1359, H1755, H1437, and H1792 cells were maintained in RPMI1640 (Mediatech) supplemented with 10% FBS. Immortalized human lung airway epithelial (AALE) cells (32) were maintained in SABM supplemented with SAGM SingleQuots (Lonza). Retroviruses were produced by transfecting 293T packaging cells with pBabe/pWzl/pMKO and pCL-Ampho plasmids (51). Lentiviruses were produced by transfecting 293T packaging cells with a 3-plasmid system (30). To generate stable cell lines, cells were selected in media containing 2 μg/mL puromycin for 2 days or 10 μg/mL blasticidin for 4 days.

Chemicals

Gefitinib, dasatinib, and GDC-0941 were purchased from Selleck Chemicals. PHA665752 was purchased from Tocrus Biosciences. LY294002 was purchased from EMD Biosciences.

Cell Proliferation Assay

Cells were seeded into 96-well plates for 24 hours. Six replicate infections were performed for control shRNAs or each gene-specific shRNA in the presence of 4 μg/mL polybrene for 24 hours followed by selection in media containing 2 μg/mL puromycin. The ATP content was measured at 5 days by use of the CellTiter-Glo luminescent cell viability assay (Promega). Data represent mean ± SD of 6 replicate measurements.

For the rescue experiments, H1755 (1.8×10^5) cells were incubated with lentiviruses expressing LacZ control, CRKL, RAP1, RAP1A^{63E}, RAP1B, or RAP1B^{V12} in 24-well plates in the presence of 4 μg/mL polybrene and spin-infected at 1,000 × *g* for 2 hours at 37°C. Cells were then trypsinized and replated at a density of 1,500 cells/well in 96-well plates for 24 hours.

For measuring IC_{50}, HCC827 cells (1.5×10^3) expressing CRKL or a control vector were seeded into 96-well plates for 24 hours and then incubated with gefitinib for 72 hours. The ATP content was measured by use of the CellTiter-Glo luminescent cell viability assay (Promega). Data represent mean ± SD relative to untreated cells for each cell line. For the RNAi experiments, HCC827 cells overexpressing CRKL or a control vector were infected with lentiviruses encoding indicated shRNAs for 24 hours, and then selected with 2 μg/mL puromycin for 2 days. Cells were replated into 96-well plates for 24 hours before treatment with gefitinib for 72 hours.

Luminex Immunosandwich Assay

AALE (1.5×10^5) cells were plated onto each well of 6-well plates for 24 hours. Triplicate transfections with 3 μg of pLenti-LacZ, CRKL, or CRKL^{W160L} were performed with FuGENE 6 (Roche) for 16 hours. After the incubation, medium was replaced with fresh medium and cells were cultured for another 32 hours before collecting cell lysates. The Luminex immunosandwich assay was performed as described (45).

Anchorage-Independent Growth Assay

Growth in soft agar was determined by plating 5×10^4 cells in triplicate in 0.4% Noble agar (51). Colonies greater than 0.2 mm in diameter were counted 4 weeks after plating. Data represent mean ± SD of 6 replicate measurements from 2 independent experiments.

Tumorigenicity Assay

Tumor xenograft experiments were performed as described (51). AALE cells expressing the indicated constructs were trypsinized and collected in DMEM supplemented with 10% FBS. Cells (8×10^6) were resuspended in 400 μL of 1× PBS and mixed with 400 μL of Matrigel-Basement Membrane Matrix, LDEV-free (BD Biosciences). The cell mixture (200 μL, containing 2×10^6 cells) was injected subcutaneously into 6-week-old male BALB/c nude mice (Charles River). Tumor injection sites were monitored for 5 months.

For tumor growth studies, HCC515 cells were infected with lentiviruses expressing luciferase followed by selection in media containing 10 μg/mL blasticidin for 5 days. Luciferized HCC515 cells were transduced with lentiviruses encoding pLKO-Tet-On-scrambled control shRNA or pLKO-Tet-On-shCRKL#1 and selected in 2 μg/mL puromycin to generate stable cell lines. Cells (5×10^6) were resuspended in 200 μL of PBS and injected subcutaneously into 6-week-old male BALB/c nude mice (Charles River). Tumor size was measured twice weekly by a caliper. Noninvasive bioluminescent imaging was performed at 11 and 32 days after implantation. Mice were given a single intraperitoneal injection of a mixture of luciferin (50 mg/kg), ketamine (150 mg/kg), and xylazine (12 mg/kg) in sterile water. After 5 minutes, mice were placed in a chamber and photons were captured for a time period of 120 seconds with an IVIS imaging camera (Xenogen). Images were generated by the use of LIVING IMAGE 2.60.1 software.

Immunoblotting

Cell lysates were prepared by scraping cells in lysis buffer (50 mM Tris, (pH 8; 150 mM NaCl; 1% Nonidet P40; 0.5% sodium deoxycholate; and 0.1% sodium dodecyl sulfate) containing complete protease inhibitors (Roche) and phosphatase inhibitors (10 mM sodium fluoride and 5 mM sodium orthovanadate). Protein concentration was measured by use of the BCA Protein Assay kit (Pierce). An equal amount of protein (30 μg) was separated by NuPAGE Novex Bis-Tris 4%–12% gradient gels (Invitrogen) and then transferred onto a polyvinylidene difluoride membrane (Amersham). The membrane was then incubated with primary antibodies for 1 hour at room temperature. Phospho-specific antibodies against phospho-S473 AKT (#9271), phospho-Y1068 EGFR (#3777), phospho-Y1289 ERBB3 (#4791), phospho-T202/Y204 ERK1/2 (#4370), phospho-Y118 Paxillin (#2541), phospho-S338 RAF1 (#9427), and phospho-Y416 SRC (#2113) were purchased from Cell Signaling. Antibodies against ERK1/2 (#4695), ARAF (#4432), RAF1 (#9422), Caspase-3 (#9662), and PARP (#9532) were purchased from Cell Signaling Technology. Antibodies against BRAF (sc-5284), phospho-Y504 C3G (sc-12926), C3G (sc-869), CRKL (sc-319), KRAS (sc-30), SOS1 (sc-256), and SRC (sc-19) were from Santa Cruz Biotechnology, Inc. Antibodies against phospho-Y249 p130CAS (#558401) and p130CAS (#610272) were from BD Biosciences. Antibodies against p85 (#06-496), RAS (#05-516), RAP1 (#07-916), phospho-MEK (#07-461), and phosphotyrosine (4G10) were from Millipore. Antibody specific for NF1 was provided by Karen Cichowski, Brigham and Women's Hospital.

After incubation with the appropriate horseradish peroxidase-linked secondary antibodies (Bio-Rad), signals were visualized by enhanced chemiluminescence plus Western blotting detection reagents (Amersham). Expression of β-actin was also assessed as an internal loading control by the use of a specific antibody (sc-8432-HRP; Santa Cruz Biotechnology, Inc.). Intensities of bands were quantified by LabWorks image analysis software (UVP).

Immunoprecipitation

Cell lysates were collected by scraping cells in immunoprecipitation buffer (20 mM Tris, pH 8; 100 mM NaCl; 2 mM EDTA; and 0.5% NP-40) containing protease and phosphatase inhibitors. Protein extracts (1 mg) were incubated with 2 μg of anti-CRKL antibody (sc-319;Santa Cruz Biotechnology, Inc.), 5 μg of anti-p85 antibody (#06-496; Millipore), or normal Rabbit IgG (sc-2070; Santa Cruz Biotechnology, Inc.) for 2 hours at 4°C followed by incubation with 30 μL of Protein A/G-PLUS agarose beads (sc-2003; Santa Cruz Biotechnology, Inc.) for 1 hour at 4°C. Beads were collected by centrifugation at 2,000 × g for 3 min at 4°C and resuspended in 1 mL of immunoprecipitation buffer

for washing. After 4 repeats of washing and centrifugation, beads were boiled for 5 minutes in 1× NuPAGE LDS sample buffer (Invitrogen).

The pull-down assay for GTP-bound RAS or RAP1 was performed by the use of RAS and RAP1 activation assay kits (Millipore), respectively. For measuring *in vitro* BRAF kinase activity, 500 μg of protein extracts was incubated with 2 μg of anti-BRAF antibody (sc-5284; Santa Cruz Biotechnology, Inc.) or normal mouse IgG (sc-2025; Santa Cruz Biotechnology, Inc.) for 2 hours at 4°C followed by incubation with 20 μL of Protein A/G-Plus agarose beads for 1 hour at 4°C. After 5 washes with immunoprecipitation buffer, the beads were incubated with 1.34 μg of MEK substrate proteins (#17-359; Millipore) in the presence of 37.5 mM $MgCl_2$ and 250 μM ATP for 30 minutes at 30°C. The beads were boiled in sample buffer for 5 minutes, and the supernatants were resolved for immunoblotting for phospho-MEK1 (#07-461; Millipore).

Real-Time Quantitative Reverse-Transcription PCR

Total RNA was extracted with TRIzol reagent (Invitrogen) and 1 μg of total RNA was used to synthesize the first-strand cDNA using Oligo$(dT)_{20}$/random hexamer primer cocktails and Superscript III reverse transcriptase (Invitrogen). Quantitative PCRs were performed with the use of SYBR green PCR Master Mix (Applied Biosystems). The primer sequences used are as follows: *CRKL*-primer set 1 (forward: 5′-CTGTCGGTGTCCGAGAACTC-3′; reverse: 5′-ATTGGTGGGCTTGGATACCTG-3′), *CRKL*-primer set 2 (forward: 5′-AAGCCCACCAATGGGATCTG-3′; reverse: 5′-ACTCCACCACT GTTCTTCAGG-3′), and *GAPDH* (forward: 5′-CCTGTTCGACAGTCA GCCG-3′; reverse: 5′-CGACCAAATCCGTTGACTCC-3′). Triplicate reactions were performed separately on the same cDNA samples by use of the ABI 7900HT real-time PCR instrument (Applied Biosystems). The mean cycle threshold was used for the comparative cycle threshold analysis method (ABI User Bulletin #2; http://www3.appliedbiosystems.com/cms/groups/mcb_support/documents/generaldocuments/cms_040980.pdf).

Quantitative PCR for Gene Copy Number

The standard curve method was used to determine the copy number of *CRKL* in NSCLC and AALE cells. Genomic DNA was extracted by use of the DNeasy blood and tissue kit (QIAGEN). The primer sequences for detecting *CRKL* were 5′-TTGACAGGCACTGGCTTAGA-3′ and 5′-GGCACTCCACCACTGTTCTT-3′. The primer sequences for detecting *LINE-1* were 5′-AAAGCCGCTCAACTACATGG-3′ and 5′-TGCTTTGAATGCGTCCCAGAC-3′. The standard curve was generated by PCR of serially diluted genomic DNA of AALE cells (50, 10, 2, 0.4, and 0.08 ng). Triplicate reactions were performed by the use of 2 ng of genomic DNA extracted from NSCLC cells. The gene copy number was normalized to *LINE-1* and normal reference DNA of AALE cells.

Fluorescence In Situ *Hybridization*

The BAC RP11-505B16 clone containing CRKL (Invitrogen) was labeled with digoxigenin (Roche) and the BAC RP11-47N6 clone containing 22q13.2 as a reference (Invitrogen) was labeled with biotin using the BioPrime labeling mix (Invitrogen). Labeled DNA was precipitated at −80°C for 2 hours with glycogen (20 μg/μL), pelleted by centrifugation at 18,000 × *g* for 15 minutes at 4°C, air-dried for 10 minutes, and resuspended in 50 μL of hybridization buffer (50% deionized formamide, 10% dextran sulfate, 2× SSC).

Slides containing metaphase chromosomes were pretreated with 1:25 Digest-All III (Invitrogen) at 37°C for 6 minutes and fixed in 10% buffered formalin for 1 minute. Slides were dehydrated for 2 minutes each in 70%, 90%, and 100% ethanol. Probes were prepared by mixing 2 μL of each labeled probe, 1 μL of Cot-1 DNA (1 mg/mL; Invitrogen), and 11 μL of hybridization buffer. Probes were applied to air-dried slides and covered with coverslips. Slides were incubated at 72°C for 5 minutes to denature probes. Hybridization was performed for 18 hours at 37°C in a dark, humid chamber. After hybridization, slides were washed in 0.5× SSC at 72°C for 5 minutes and rinsed in PBS containing 0.025% Tween-20 at room temperature. Slides were blocked with CAS-Block containing 10% normal goat serum (Invitrogen) and incubated with FITC-anti-digoxigenin (Roche) and Alexa Fluor 594 Streptavidin (Invitrogen). Slides were washed in PBS containing 0.025% Tween-20 and counterstained with DAPI (Invitrogen). Images were captured with the use of a Zeiss Axio Observer Z1 microscope and AxioVision imaging software (Zeiss).

Tumor specimens from erlotinib-treated patients were obtained from Dana-Farber Cancer Institute, Brigham and Women's Hospital, and Massachusetts General Hospital. All samples were analyzed under Institutional Review Board-approved protocols. The presence of *EGFR* mutations in each specimen was confirmed as described (54, 55). FISH analysis of tumor specimens with a *CRKL*-specific probe (BAC RP11-505B16) and a chromosome 22 telomere-specific probe (Abbott Molecular) were performed as described previously (54).

Disclosure of Potential Conflicts of Interest

W.C. Hahn and M. Meyerson are consultants for Novartis Pharmaceuticals; P.A. Jänne is a consultant for Roche, Genentech, Astra-Zeneca, Boehringer Ingelheim, and Pfizer. No other potential conflicts of interest were disclosed.

Acknowledgments

We thank Karen Cichowski, Heidi Greulich, Guo Wei, and Gromoslaw Smolen for reagents and cell lines; Ronny Drapkin, Lynette Sholl, Craig Mermel, Rameen Beroukhim, Milan Chheda, Susan Moody, and David Barbie for helpful discussions; and Qi Wang, Laura Johnson, and Sapana Thomas for technical assistance.

Grant Support

This work was supported in part by grants from the National Institutes of Health (R33 CA128625, U54 CA112962, R01 CA135257, R01 CA114465, P50 CA090578).

Received March 4, 2011; revised September 23, 2011; accepted October 6, 2011; published OnlineFirst October 17, 2011.

REFERENCES

1. Pao W, Miller V, Zakowski M, Doherty J, Politi K, Sarkaria I, et al. EGF receptor gene mutations are common in lung cancers from "never smokers" and are associated with sensitivity of tumors to gefitinib and erlotinib. Proc Natl Acad Sci U S A 2004;101:13306–11.
2. Rosell R, Moran T, Queralt C, Porta R, Cardenal F, Camps C, et al. Screening for epidermal growth factor receptor mutations in lung cancer. N Engl J Med 2009;361:958–67.
3. Mitsudomi T, Morita S, Yatabe Y, Negoro S, Okamoto I, Tsurutani J, et al. Gefitinib versus cisplatin plus docetaxel in patients with non–small-cell lung cancer harbouring mutations of the epidermal growth factor receptor (WJTOG3405): an open label, randomised phase 3 trial. Lancet Oncol 2010;11:121–8.
4. Maemondo M, Inoue A, Kobayashi K, Sugawara S, Oizumi S, Isobe H, et al. Gefitinib or chemotherapy for non–small-cell lung cancer with mutated EGFR. N Engl J Med 2010;362:2380–8.
5. Lynch TJ, Bell DW, Sordella R, Gurubhagavatula S, Okimoto RA, Brannigan BW, et al. Activating mutations in the epidermal growth factor receptor underlying responsiveness of non–small-cell lung cancer to gefitinib. N Engl J Med 2004;350:2129–39.

6. Paez JG, Janne PA, Lee JC, Tracy S, Greulich H, Gabriel S, et al. EGFR mutations in lung cancer: correlation with clinical response to gefitinib therapy. Science 2004;304:1497–500.
7. Mok TS, Wu YL, Thongprasert S, Yang CH, Chu DT, Saijo N, et al. Gefitinib or carboplatin-paclitaxel in pulmonary adenocarcinoma. N Engl J Med 2009;361:947–57.
8. Soda M, Choi YL, Enomoto M, Takada S, Yamashita Y, Ishikawa S, et al. Identification of the transforming EML4-ALK fusion gene in non-small-cell lung cancer. Nature 2007;448:561–6.
9. Shaw AT, Yeap BY, Mino-Kenudson M, Digumarthy SR, Costa DB, Heist RS, et al. Clinical features and outcome of patients with non-small-cell lung cancer who harbor EML4-ALK. J Clin Oncol 2009;27:4247–53.
10. Kwak EL, Bang YJ, Camidge DR, Shaw AT, Solomon B, Maki RG, et al. Anaplastic lymphoma kinase inhibition in non-small-cell lung cancer. N Engl J Med 2010;363:1693–703.
11. McDermott U, Iafrate AJ, Gray NS, Shioda T, Classon M, Maheswaran S, et al. Genomic alterations of anaplastic lymphoma kinase may sensitize tumors to anaplastic lymphoma kinase inhibitors. Cancer Res 2008;68:3389–95.
12. Weir BA, Woo MS, Getz G, Perner S, Ding L, Beroukhim R, et al. Characterizing the cancer genome in lung adenocarcinoma. Nature 2007;450:893–8.
13. Beroukhim R, Getz G, Nghiemphu L, Barretina J, Hsueh T, Linhart D, et al. Assessing the significance of chromosomal aberrations in cancer: methodology and application to glioma. Proc Natl Acad Sci U S A 2007;104:20007–12.
14. Kendall J, Liu Q, Bakleh A, Krasnitz A, Nguyen KC, Lakshmi B, et al. Oncogenic cooperation and coamplification of developmental transcription factor genes in lung cancer. Proc Natl Acad Sci U S A 2007;104:16663–8.
15. Kwei KA, Kim YH, Girard L, Kao J, Pacyna-Gengelbach M, Salari K, et al. Genomic profiling identifies TITF1 as a lineage-specific oncogene amplified in lung cancer. Oncogene 2008;27:3635–40.
16. Zhao X, Weir BA, LaFramboise T, Lin M, Beroukhim R, Garraway L, et al. Homozygous deletions and chromosome amplifications in human lung carcinomas revealed by single nucleotide polymorphism array analysis. Cancer Res 2005;65:5561–70.
17. Kim YH, Kwei KA, Girard L, Salari K, Kao J, Pacyna-Gengelbach M, et al. Genomic and functional analysis identifies CRKL as an oncogene amplified in lung cancer. Oncogene 2010;29:1421–30.
18. Bass AJ, Watanabe H, Mermel CH, Yu S, Perner S, Verhaak RG, et al. SOX2 is an amplified lineage-survival oncogene in lung and esophageal squamous cell carcinomas. Nat Genet 2009;41:1238–42.
19. Beroukhim R, Mermel CH, Porter D, Wei G, Raychaudhuri S, Donovan J, et al. The landscape of somatic copy-number alteration across human cancers. Nature 2010;463:899–905.
20. Feller SM. Crk family adaptors-signalling complex formation and biological roles. Oncogene 2001;20:6348–71.
21. Birge RB, Kalodimos C, Inagaki F, Tanaka S. Crk and CrkL adaptor proteins: networks for physiological and pathological signaling. Cell Commun Signal 2009;7:13.
22. Feller SM, Knudsen B, Hanafusa H. Cellular proteins binding to the first Src homology 3 (SH3) domain of the proto-oncogene produce c-Crk indicate Crk-specific signaling pathways. Oncogene 1995;10:1465–73.
23. Sattler M, Salgia R, Shrikhande G, Verma S, Pisick E, Prasad KVS, et al. Steel factor induces tyrosine phosphorylation of CRKL and binding of CRKL to a complex containing c-Kit, phosphatidylinositol 3-kinase, and $p120^{CBL}$. J Biol Chem 1997;272:10248–53.
24. Nichols GL, Raines MA, Vera JC, Lacomis L, Tempst P, Golde DW. Identification of CRKL as the constitutively phosphorylated 39-kD tyrosine phosphoprotein in chronic myelogenous leukemia cells. Blood 1994;84:2912–8.
25. Oda T, Heaney C, Hagopian JR, Okuda K, Griffin JD, Druker BJ. Crkl is the major tyrosine-phosphorylated protein in neutrophils from patients with chronic myelogenous leukemia. J Biol Chem 1994;269:22925–8.
26. Senechal K, Heaney C, Druker B, Sawyers CL. Structural requirements for function of the Crkl adapter protein in fibroblasts and hematopoietic cells. Mol Cell Biol 1998;18:5082–90.
27. Senechal K, Halpern J, Sawyers CL. The CRKL adaptor protein transforms fibroblasts and functions in transformation by the BCR-ABL oncogene. J Biol Chem 1996;271:23255–61.
28. Schonherr C, Yang HL, Vigny M, Palmer RH, Hallberg B. Anaplastic lymphoma kinase activates the small GTPase Rap1 via the Rap1-specific GEF C3G in both neuroblastoma and PC12 cells. Oncogene 2010;29:2817–30.
29. De Falco V, Castellone MD, De Vita G, Cirafici AM, Hershman JM, Guerrero C, et al. RET/papillary thyroid carcinoma oncogenic signaling through the Rap1 small GTPase. Cancer Res 2007;67:381–90.
30. Luo B, Cheung HW, Subramanian A, Sharifnia T, Okamoto M, Yang X, et al. Highly parallel identification of essential genes in cancer cells. Proc Natl Acad Sci U S A 2008;105:20380–5.
31. Sos ML, Michel K, Zander T, Weiss J, Frommolt P, Peifer M, et al. Predicting drug susceptibility of non-small cell lung cancers based on genetic lesions. J Clin Invest 2009;119:1727–40.
32. Lundberg AS, Randell SH, Stewart SA, Elenbaas B, Hartwell KA, Brooks MW, et al. Immortalization and transformation of primary human airway epithelial cells by gene transfer. Oncogene 2002;21:4577–86.
33. Weinstein IB. Cancer. Addiction to oncogenes—the Achilles heal of cancer. Science 2002;297:63–4.
34. de Jong R, ten Hoeve J, Heisterkamp N, Groffen J. Tyrosine 207 in CRKL is the BCR/ABL phosphorylation site. Oncogene 1997;14:507–13.
35. Tanaka S, Morishita T, Hashimoto Y, Hattori S, Nakamura S, Shibuya M, et al. C3G, a guanine nucleotide-releasing protein expressed ubiquitously, binds to the Src homology 3 domains of CRK and GRB2/ASH proteins. Proc Natl Acad Sci U S A 1994;91:3443–7.
36. Gotoh T, Hattori S, Nakamura S, Kitayama H, Noda M, Takai Y, et al. Identification of Rap1 as a target for the Crk SH3 domain-binding guanine nucleotide-releasing factor C3G. Mol Cell Biol 1995;15:6746–53.
37. Nosaka Y, Arai A, Miyasaka N, Miura O. CrkL mediates Ras-dependent activation of the Raf/ERK pathway through the guanine nucleotide exchange factor C3G in hematopoietic cells stimulated with erythropoietin or interleukin-3. J Biol Chem 1999;274:30154–62.
38. Smit L, van der Horst G, Borst J. Sos, Vav, and C3G participate in B cell receptor-induced signaling pathways and differentially associate with Shc-Grb2, Crk and Crk-L adaptors. J Biol Chem 1996;271:8564–9.
39. Vossler MR, Yao H, York RD, Pan MG, Rim CS, Stork PJ. cAMP activates MAP kinase and Elk-1 through a B-Raf- and Rap1-dependent pathway. Cell 1997;89:73–82.
40. York RD, Yao H, Dillon T, Ellig CL, Eckert SP, McCleskey EW, et al. Rap1 mediates sustained MAP kinase activation induced by nerve growth factor. Nature 1998;392:622–6.
41. Bouschet T, Perez V, Fernandez C, Bockaert J, Eychene A, Journot L. Stimulation of the ERK pathway by GTP-loaded Rap1 requires the concomitant activation of Ras, protein kinase C, and protein kinase A in neuronal cells. J Biol Chem 2003;278:4778–85.
42. Ohtsuka T, Shimizu K, Yamamori B, Kuroda S, Takai Y. Activation of brain B-Raf protein kinase by Rap1B small GTP-binding protein. J Biol Chem 1996;271:1258–61.
43. Akagi T, Shishido T, Murata K, Hanafusa H v-Crkactivates the phosphoinositide 3-kinase/AKT pathway in transformation. Proc Natl Acad Sci U S A 2000;97:7290–5.
44. Stam JC, Geerts WJ, Versteeg HH, Verkleij AJ, van Bergen en Henegouwen PM. The v-Crk oncogene enhances cell survival and induces activation of protein kinase B/Akt. J Biol Chem 2001;276:25176–83.
45. Du J, Bernasconi P, Clauser KR, Mani DR, Finn SP, Beroukhim R, et al. Bead-based profiling of tyrosine kinase phosphorylation identifies SRC as a potential target for glioblastoma therapy. Nat Biotechnol 2009;27:77–83.

46. Fukuyama T, Ogita H, Kawakatsu T, Fukuhara T, Yamada T, Sato T, et al. Involvement of the c-Src-Crk-C3G-Rap1 signaling in the nectin-induced activation of Cdc42 and formation of adherens junctions. J Biol Chem 2005;280:815–25.
47. Matsuda M, Hashimoto Y, Muroya K, Hasegawa H, Kurata T, Tanaka S, et al. CRK protein binds to two guanine nucleotide-releasing proteins for the Ras family and modulates nerve growth factor-induced activation of Ras in PC12 cells. Mol Cell Biol 1994;14:5495–500.
48. Hamad NM, Elconin JH, Karnoub AE, Bai W, Rich JN, Abraham RT, et al. Distinct requirements for Ras oncogenesis in human versus mouse cells. Genes Dev 2002;16:2045–57.
49. Rangarajan A, Hong SJ, Gifford A, Weinberg RA. Species- and cell type-specific requirements for cellular transformation. Cancer Cell 2004;6:171–83.
50. Boehm JS, Hession MT, Bulmer SE, Hahn WC. Transformation of human and murine fibroblasts without viral oncoproteins. Mol Cell Biol 2005;25:6464–74.
51. Boehm JS, Zhao JJ, Yao J, Kim SY, Firestein R, Dunn IF, et al. Integrative genomic approaches identify *IKBKE* as a breast cancer oncogene. Cell 2007;129:1065–79.
52. Ding L, Getz G, Wheeler DA, Mardis ER, McLellan MD, Cibulskis K, et al. Somatic mutations affect key pathways in lung adenocarcinoma. Nature 2008;455:1069–75.
53. Thomas RK, Baker AC, Debiasi RM, Winckler W, Laframboise T, Lin WM, et al. High-throughput oncogene mutation profiling in human cancer. Nat Genet 2007;39:347–51.
54. Engelman JA, Zejnullahu K, Mitsudomi T, Song Y, Hyland C, Park JO, et al. MET amplification leads to gefitinib resistance in lung cancer by activating ERBB3 signaling. Science 2007;316:1039–43.
55. Sequist LV, Waltman BA, Dias-Santagata D, Digumarthy S, Turke AB, Fidias P, et al. Genotypic and histological evolution of lung cancers acquiring resistance to EGFR inhibitors. Sci Transl Med 2011;3:75ra26.